Dynamics of Energy Transfer in Light Harvesting Photosynthetic Systems

P. Molukanele

21183406

Dissertation submitted in fulfilment of the requirements for the degree *Master of Science*

at the Potchefstroom Campus of the North-West University

NORTH-WEST UNIVERSITY
YUNIBESITI YA BOKONE-BOPHIRIMA
NOORDWES-UNIVERSITEIT

Supervisor: **Prof. L. van Rensburg**

Co-Supervisor: **Dr. R. Sparrow**

September 2009

Declaration

I, Palesa Molukanele, declare herewith that the dissertation entitled, "Dynamics of energy transfer in light harvesting photosynthetic systems", which I herewith submit to the North- West University in fulfilment of the requirements set for the Master of Science degree, is my own work and has not already been submitted to any other university.

Signature of Student: ....Rmala.....

Date: .....20|08|2009.....

Abstract

Photosynthesis is the process by which plants, algae and photosynthetic bacteria convert sunlight energy into chemical energy (ATP). The initial stages of this process (harvesting solar energy and transferring it to the reaction centres) occur extremely fast and with an efficiency of close to 100%. Studying the dynamics of these reactions will enable us to develop artificial functional light harvesting arrays and energy transfer systems that mimic the process in nature, thus helping us use light as an energy source that is environmentally clean, efficient, sustainable and carbon-neutral. These reactions can be measured using femtosecond pump-probe spectroscopy (transient absorption in the liquid phase and monitoring the subsequent kinetics in the wavelength region: 400 nm-700 nm). In order to perform these experiments, photosynthetic pigment-protein complexes must be isolated, purified and characterised. In this work, these photosynthetic complexes were isolated from spinach leaves and characterised using various biological and spectroscopic techniques. Finally, the first results of pump-probe application to biological samples in South Africa were discussed.

Opsomming

Fotosintese is die proses waardeur plante, alge en fotosinterende bakterieë sonlig omskep in chemiese energie (ATP). Die aanvanklike stappe van die proses (die absorpsie van sonlig-energie en die oordrag daarvan na die reaksiesentrums) vind baie vinnig en met 'n effektiwiteit van ongeveer 100 % plaas. Bestudering van die dinamika van die reaksies stel ons in staat om kunsmatige, funksionele lig-absorberende matrikse en energie-oordrag stelsels te ontwerp wat die natuur naboots. Dit beteken dat lig as 'n omgewingsvriendelike, effektiewe en volhoubare energiebron gebruik kan word. Om die reaksietempo's te meet word *pump-probe* spektroskopie gebruik, wat die monitering van die kinetiese reaksies in die golflengte spektrum van 400 – 700nm na absorpsie in die vloeistoffase behels. Die eksperimente vereis fotosinterende pigment-proteïen komplekse wat geïsoleerd, verfyn en gekarakteriseerd is. Vir die huidige projek is hierdie komplekse uit spinasieblare geïsoleer en gekarakteriseer deur middel van verskeie biologiese en spektroskopiese tegnieke. Die eerste *pump-probe* resultate verkry van biologiese monsters in Suid-Afrika word ook bespreek.

Acknowledgements

I am particularly grateful to my supervisor, Professor Leon van Rensburg (NWU) and co-supervisor Dr Raymond Sparrow (CSIR), for their valuable suggestions and relentless efforts which have made this work possible. Under their supervision and direction the quality of this work improved significantly.

I would also like to express much gratitude and appreciation to the following people who assisted me in one way or the other during the course of the project work.

- Dr Isak Gerber (CSIR-Biosciences) for giving me training on how to make good gels and giving me valuable lab guidance.

- Mr Saturnin Ombinda-Lemboumba (CSIR-NLC) for his utmost assistance and for taking care of all the physics (laser) involved in this work.

- Dr Lourens Botha and Dr Anton du Plessis (Competency Area Manager and Project Leader – NLC) respectively for their guidance and assistance in all aspect of this project.

- Mr Hendrik Maat (CSIR-NLC) for all the technical support when working in the femtosecond lab.

- Dr Suretha Potgieter (CSIR- Biosciences) for her assistance, love and support when doing the biological preparations.

- Ms Vatiswa Mbebe for her assistance with administration work.

- The staff and students of the CSIR (National Laser Centre, Biosciences) and North-West University for their constant words of encouragement.

- The CSIR for their financial support of the research and financial support of my well-being.

I would also like to thank my grandmother (Mrs N.M. Leroala) and my family for their encouragement throughout my life.

To Tseliso Tefo Molukanele (my husband), thank you for your love, prayers and constant support during the course of this work.

To my princess Hlompho Mosa Molukanele, thank you for giving me the motivation and inspiration to be the best I can be for you.

The greatest of all the thanksgiving goes to God Almighty, for giving me the strength and energy throughout the course of this study.

Table of Contents

Glossary of terms

PS:	Photosystem
LHC:	Light harvesting complex
LH:	Light harvesting
RC/RCs:	Reaction centre/centres
PSU:	Photosynthetic unit
ATP:	Adenosine Tri-phosphate
NADP:	Nicotinamide adenine dinucleotide phosphate
CD:	Circular Dichroism
Chl:	Chlorophyll
BChl:	Bacteriochlorophyll
BPh:	Bacteriopheophytin
Lut:	Luteins
Neo:	Neoxanthin
Vio:	Violaxanthin
Fd:	Ferredoxin
fs:	Femtosecond ($1x\ 10^{-15}$)
ps:	Picosecond (1×10^{-12})
ns:	Nanosecond (1×10^{-9})
CO_2:	Carbon dioxide
O_2:	Oxygen
$C_6H_{12}0_6$:	Sugar (Glucose)
H_20:	Water molecule
CSIR:	Council for Scientific and Industrial Research
NLC:	National Laser Centre
NWU:	North-West University
Eqn:	Equation
Rps. Viridis:	Rhodopseudomonas viridis
MW:	Molecular weight

CHAPTER 1

Introduction

Through photosynthesis, green plants, photosynthetic bacteria and cyanobacteria are able to absorb solar energy and store it by a series of events that eventually converts it into biochemical energy [Engel et al., 2007]. In green plants and algae, the primary reactions of this process (energy transfer processes) occur in the thylakoid membranes. These systems are highly organised and host the antenna complexes that transfer absorbed light energy to the reaction centre (RC) surrounding them, where the redox reactions are initiated and subsequently the formation of Adenosine Tri-phosphate (ATP) which is the energy storing molecule, takes place [van Oort, 2007] [Van Grondelle et al., 1994].

The transfer of the excitation energy from the antenna complexes to the RC takes place almost instantaneously, from a few femtoseconds (fs) to many nanoseconds (ns) so little energy is wasted as heat, and this occurs with an efficiency of nearly 100%. How photosynthesis achieves this near instantaneous energy transfer, is a topic that is still under investigation [Engel et al., 2007].

1.1 Background to the project

Research has been performed on the antenna complexes of both photosynthetic bacteria and higher plants; from discovering the structures of these complexes [(Kuhlbrandt et al., 1994), (Liu et al., 2004)], to the time it takes the energy to migrate from the complexes to the reaction centres. However the understanding of the high efficiency of these processes is still being studied today.

Although the atomic-scale structures of the light harvesting complexes [Liu et al., 2004)] and the reaction centres (RCs) [Ferreira et al., 2004] are known and have been predicted to assemble in a certain way in the photosynthetic unit (PSU), a detailed assembly of the PSU, which consists of the light harvesting complexes and the reaction centres, is not known, and hence it is difficult to assess the importance of structural features from the point of view of overall performance and function.

Concomitantly, in order to interpret and understand the spectroscopic and dynamic data in terms of a detailed molecular level reaction mechanism, atomic-scale structural information is required, and is available for many photosynthetic organisms, therefore many researchers, such as Engel et al., 2007, have attempted to monitor the reaction mechanism (energy pathways) using spectroscopic methods.

1.2 Motivation of the project

Light harvesting and energy transfer processes of photosynthesis are among the fastest and most efficient processes in nature, and understanding the dynamics of these processes can contribute to the knowledge base of research and provide an insight into how nature operates.

Learning enough about the energy transfer processes, might enable many researchers to develop artificial, functional light harvesting arrays of photosynthesis that could help in an attempt to effectively use the sun as a clean, efficient, sustainable and carbon-neutral source of energy. This may hugely benefit society.

The main reason for this research is to develop artificial, functional light harvesting arrays and energy transfer systems that mimic the process in nature. Light harvesting preparations from spinach leaves, which assisted in calibrating and benchmarking the femtosecond pump-probe transient absorption system currently installed at the National Laser Centre (NLC) laboratories, were used to perform preliminary experiments working towards the main goal.

This research is on going in the many parts of the world such as the US as well as Europe (Amsterdam), but little research has been carried out in Africa regarding this aspect of photosynthesis, and this is why this study is important.

1.3 Objectives of the project

The main objective of the overall project is to investigate the dynamics of energy transfer over a timescale that extends from several tens of fs to many ns, and this is achieved by using the femtosecond laser technique (pump-probe transient absorption spectroscopy).

In order to achieve this, photosynthetic pigment-protein complexes, such as Photosystems I and II, and the light harvesting complexes to be used for the pump-probe experiments, must be isolated, purified and characterised. This process is not easy since these are biological components and are sensitive to *in vitro* conditions; hence, the objective of this research is to prepare these photosynthetic complexes.

This is a collaborative project between the National Laser Centre (Laser sources group) and the newly established ERA (Emerging Research Area) of Synthetic Biology and collaborator at the North-West University (Potchefstroom Campus).

This is an interdisciplinary research project aimed at the establishment of a world-class ultra-fast (femtosecond) pump-probe transient absorption system. The NLC was responsible for the laser physics aspects of this project under the management of the CAM (Competence Area Manager-Dr. Lourens Botha). Dr. Anton du Plessis (Research group leader) took the daily on-going responsibility for the direction of the experimental setup along with Saturnin Ombinda (a laser physics PhD student). All the biological preparations were performed at the Council for Scientific and Industrial Research (CSIR)-Biosciences, under the supervision of Dr. Raymond Sparrow.

1.4 Dissertation layout

The work conducted during this project is presented in six chapters. The first chapter introduces the research conducted; this outlines the background to the project, the study motivation as well as the objectives of this project. The second chapter is the literature review, illustrating the work that has been performed in this field of study by other researchers. Chapter 3 discusses the background to the techniques used to characterise the extracted sample. The experimental techniques used to conduct this research are outlined in Chapter 4. The results obtained from the experiments are presented and discussed in Chapter 5. Conclusions drawn from the results and recommendations for future work are outlined in Chapter 6.

CHAPTER 2

Literature review

2.1 What is photosynthesis?

Photosynthesis is the process by which plants, algae and photosynthetic bacteria convert sunlight energy into chemical energy. This energy, which is in the form of biomolecules, becomes available to other members of the biosphere through food chains [Garrett and Grisham, 1999]. Photosynthetic organisms have an efficient system that is able to do this conversion and it is associated with the action of the green pigment called chlorophyll [Amesz, 1987; Amesz and Hoff, 1996; Baker 1996].

The overall chemical reactions of photosynthesis can be summarised as follows [Garrett & Grisham, 1999]:

$$6H_2O + 6CO_2 \text{ ----------> } C_6H_{12}O_6 + 6O_2 \qquad \textbf{(Eqn: 2.1)}$$

In photosynthetic prokaryotes and eukaryotes, this process takes place in two phases, the light reactions and the dark reactions. In green algae and plants, light reactions occur in the thylakoid membrane and converts light energy to chemical energy and hence are referred to as light dependent. The dark reactions take place in the stroma within the chloroplast, and converts CO_2 to sugar. Light is not necessary for the dark reactions to occur, and the products of the light reactions (ATP and NADPH) are used to drive the dark reactions.

The dark reactions involve a metabolic pathway called the Calvin cycle in which CO_2, NADPH and energy in the form of ATP are used to form sugars. In fact, the first product of the dark reactions of photosynthesis is a three-carbon compound called glycerol-3-phosphate, where almost immediately, two of these join to form a glucose molecule through a series of metabolic steps [Barber, 1992].

For the purpose of this study, only the first stages of the light harvesting reactions will be considered, which are the energy trapping and migration or transfer of this excitation energy.

2.1.1 Photosynthetic process location

In higher plants, photosynthesis primarily occurs in leaves. A typical plant leaf may be viewed as a solar collector full of photosynthetic cells, and contains the upper and lower epidermis (photosynthesis does not occur here because of the lack of chloroplasts), the mesophyll cells, the vascular bundles (veins) and the stomata (see Figure 2.1 below).

The stomata allow air to enter and leave the leaf (they let CO_2 in and O_2 out). Veins in a leaf are part of the plant's transportation system, moving water and nutrients around the plant as needed. The mesophyll cells contain chloroplasts and this is where photosynthesis occurs [Purves et al., (1995)].

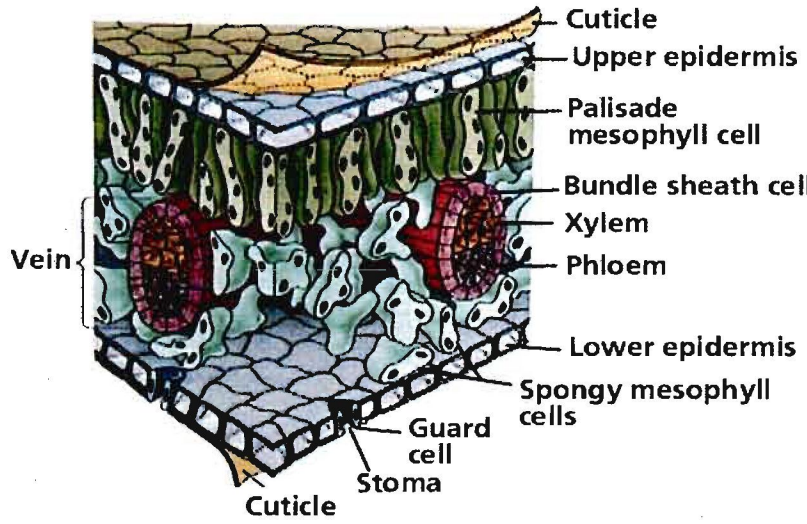

Figure 2.1: Cross section of a leaf, showing the anatomical features important to the study of photosynthesis: stoma, guard cell, mesophyll cells and vein [Purves et al., (1995)]

Chloroplasts found in the mesophyll cells contain the outer and inner membranes, intermembrane space, stroma and the thylakoids stacked in grana. Chlorophylls are situated in the membranes of the thylakoids [Staehelin, 1986] (see Figure 2.2.).

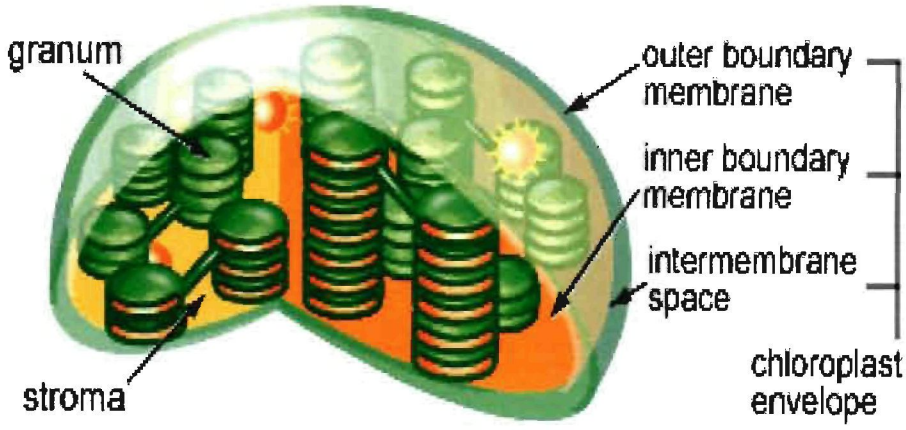

Figure 2.2: Chloroplast structure [(Campbell, 2002), (Raven et al., 1999)]

The thylakoid membrane is a complex membrane found inside the chloroplast and contains most of the proteins needed for the light reactions of photosynthesis. The required proteins for CO_2 fixation and reduction are located outside the thylakoid membrane in the surrounding aqueous phase (the stroma). Thylakoid membrane is composed mainly of glycerol lipid and protein. In this membrane, the lipid molecules arrange themselves in a bilayer (with polar head towards the water phase and the fatty acid chains inside the membrane) creating a hydrophobic core (see Figure 2.3 below).

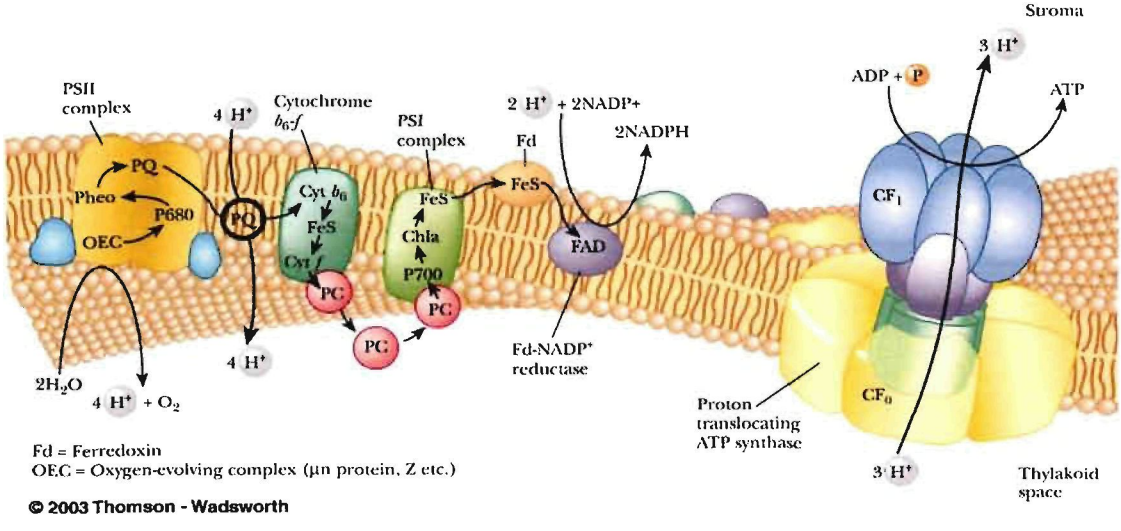

Figure 2.3: Model of the thylakoid membrane of plants illustrating the components of the electron transport chain

The thylakoid membrane is vesicular, defining a closed space with an outer aqueous space (stromal phase) and an inner space known as the thylakoid space or thylakoid lumen. The organisation of the thylakoid membrane can be described as groups of stacked membranes interconnected by non-stacked membranes that protrude from the edges of the stacks. The thylakoid membranes are continuous and the inner aqueous space of the membrane is continuous over the entire volume.

In cyanobacteria, photosynthesis takes place in granules bound to the plasma membrane. In algae, the process also takes place in chloroplasts [Berg et al., 2002].

2.2 Chlorophyll and accessory pigments

Molecules that can absorb visible light is known as a pigment. The colour of the pigment is derived from the wavelength of light not absorbed (reflected) by that specific pigment. Chlorophyll is a pigment common to all photosynthetic cells, and absorbs all wavelengths of visible light, except green. Visible light lies between wavelengths 400nm and 700nm [(Farabee, 2006), (Berg et al., 2002)]. Figure 2.4 below shows the absorption spectra of chlorophyll.

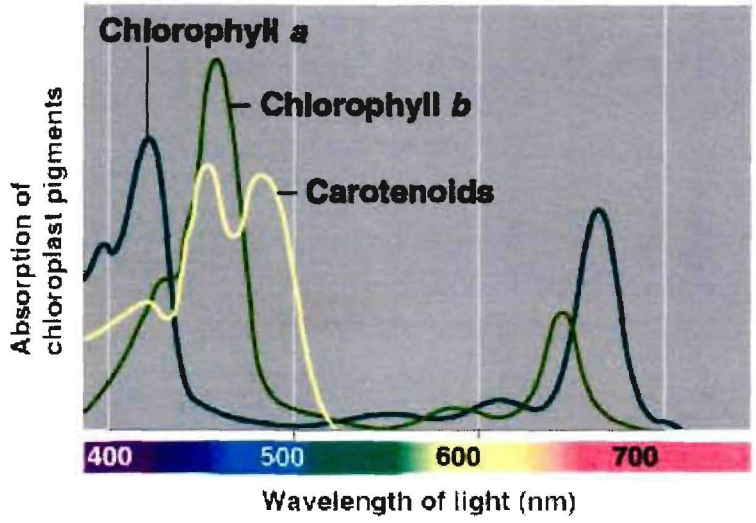

Figure 2.4: Absorption spectra of photosynthetic pigments [Auderisk and Byers, 2005]

Chlorophyll is a complex molecule and there are several modifications of this molecule occurring among plants and other photosynthetic organisms [Willstatter et al., 1928]. One type of chlorophyll, which is known as chlorophyll a, is present in all photosynthetic organisms. Other pigments, called the accessory pigments, are also present and their role is to absorb the energy not absorbed by chlorophyll a. These accessory pigments include chlorophyll b, (chlorophyll c, d and e in algae and protistans), xanthophylls and carotenoids [(Emerson & Arnold, 1932), (Ong & Tee, 1992)] (see Figure 2.4 for the absorptions spectra of some of these accessory pigments).

These pigments, together with many others, collectively form what is known as the antenna complex. In order to achieve an efficient use of light energy, photosynthetic organisms have evolved this light harvesting antenna, which allows many pigments to co-operate in the collection of light energy for a single reaction centre. In many photosynthetic systems, the size of the antenna can be adjusted to suit the light intensity [Duysens, 1952]. Chemical structures of chlorophyll a and b, and that of an accessory pigment (Beta-carotene), are shown in Figures 2.5 and 2.6 respectively.

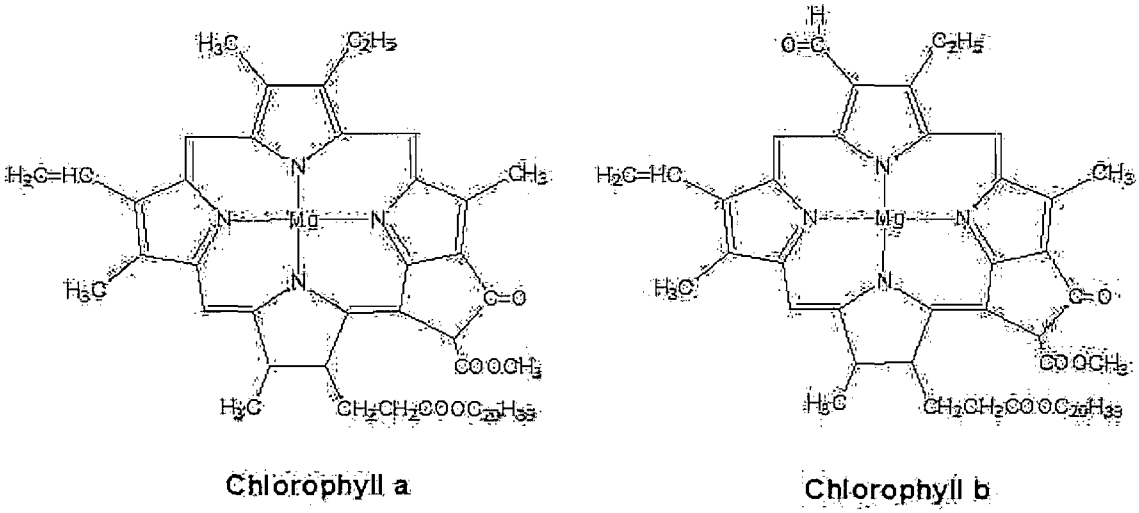

Figure 2.5: Chemical structure of chlorophyll a and b: The difference between them is the functional group (CH_3 and CHO in a and b, respectively) [Willstatter et al., 1928]

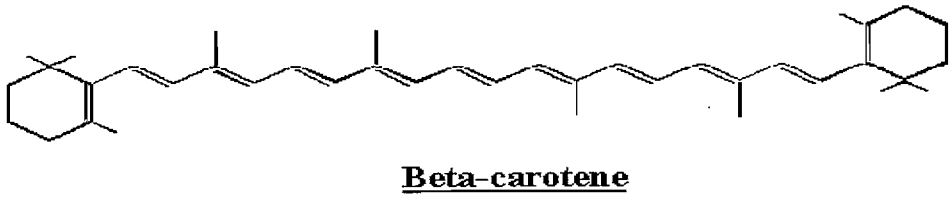

Figure 2.6: Structure of a selected carotenoid: Beta-carotene [Pfander, (1992)]

2.2.1 Absorption spectra: chlorophyll and accessory pigments

To provide energy for the process of photosynthesis, light must be absorbed by the pigments mentioned above. The light-absorbing photosynthetic pigments do not absorb all wavelengths of light equally. The absorption spectra of these pigments are shown in Figure 2.4 to illustrate this point [Auderisk and Byers, 2005].

Chlorophyll a absorbs light energy around 400-450nm and 600-700nm (from the violet-blue and orange-red wavelengths and very little from green-yellow-orange wavelengths), and chlorophyll b absorbs around 400-500nm and 630-680nm. In bacteria, bateriochlorophyll is present instead of chlorophyll and this pigment absorbs around 780nm; some absorb at longer wavelengths (870 or 1050nm) (see Figure 2.7). Wavelengths longer than 800nm are part of the infrared rather than the visible region. Carotenoids, together with chlorophyll b, absorb some of the energy in the green wavelength [(Farabee, 2006), (Berg et al., 2002].

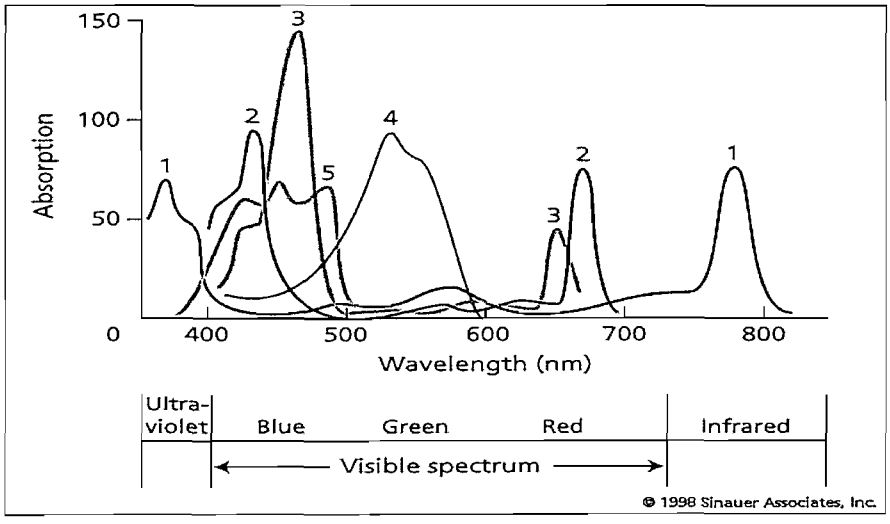

Figure 2.7: Absorption spectra of bacteriochlorophyll, chlorophyll and other accessory pigments: 1: bacteriochlorophyll, 2: chl A, 3: chl B, 4: phycoerythroblin, and 5: beta-carotene

If a pigment absorbs light energy, either one of the processes below can occur: Energy may [Farabee, 2006] [Garrett & Grisham, 1999].

- **be dissipated as heat**: energy can be lost as heat through redistribution into atomic vibrations within the pigment molecule;

- **be emitted immediately as a longer wavelength (Flourescence)**: fluorescence photon is emitted at a longer wavelength (with lower energy than the quantum of excitation), as the electron (e^-) returns to a lower state from some excited state. This fate is common in saturating light intensities;

- **Energy transduction**: transduction of light energy into chemical energy which is a photochemical event, is the essence of photosynthesis. In this case, the excited state species, by having an e^- at a higher energy level through light absorption, become a potent electron donor that can react with an e^- acceptor in its vicinity, leading to a transformation or transduction of light energy into chemical energy; or

- **Resonance energy transfer/the energy can be passed onto another molecule**: the excitation energy can be transferred by resonance energy transfer to a neighbouring molecule, if their energy level difference corresponds to the quantum of the excitation energy. In this process, the excitation energy is transferred, promoting an e^- in the receptor molecule to a higher excited energy state as the photo-excited e^- in the original absorbing molecule returns to its ground state.

In an ideal photosynthetic system, resonance energy transfer is expected to occur. Fluorescence often occurs, and this can be because of saturating light intensities as mentioned above, or because of some irregularities in the molecular organisation of the sample of interest, especially in extracted samples.

2.3 Photosystems, light harvesting complexes and the reaction centre

Generally, photosynthetic pigments are non-covalently bound to proteins, forming what is called pigment-protein complexes. These are known as light harvesting complexes, and most photosynthetic organisms contain two types, the light harvesting complex I and II (LHCI and LHCII) [Dekker and Boekema, 2004), (Zuber and Brunisholz, 1991)]. These complexes are in turn organised into what is known as Photosystem I and II (PS I and PS II), respectively. These pigment-protein complexes are organised as a photosynthetic unit (PSU) and included in the PSU are the reaction centres, which are the other type of pigment-protein complexes [Duysens, 1952]. In photosynthetic bacteria, the LHC is referred to as LH.

The main function of these light harvesting complexes is to gather light energy and to transfer it to the reaction centre for the photo-induced redox reactions. In photosynthetic bacteria, light harvesting II (LHII) is not tightly bound to the reaction centre but transfers its energy via LH I (which is tightly bound to the photosynthetic reaction centre [(Miller, 1982) (Walz and Ghosh, 1997)]), to the reaction centre [(Monger and Parson 1977), (van Grondelle et al., 1994)], see figure below.

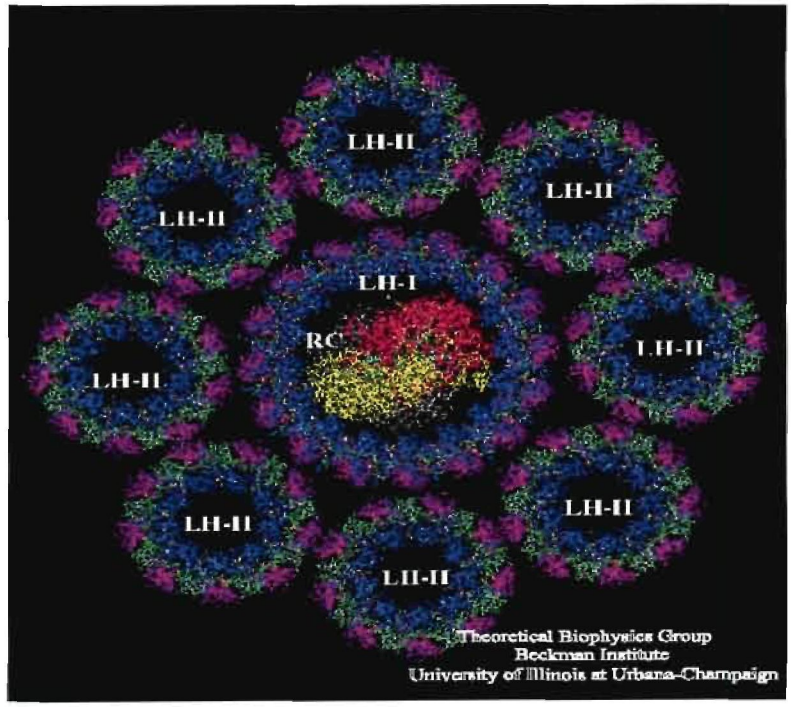

Figure 2.8: Illustrating the position of purple bacterial LHI and II around the reaction centre [Humphrey et al., 1996]

Photosystems and their associated complexes (LHC II, LHC I, reaction centres, etc.) have much information attached to them, and hence the following sections will deal with each pigment-protein complex, respectively.

2.3.1 Overview of photosystem II

Photosystem II (so called because it was the second photosystem discovered, but likely the first one evolved) [Bailey, 2006], is a large pigment-protein complex embedded in the thylakoid membranes of green plants, cyanobacteria and algae. This super complex consists of two structurally and functionally different parts: Photosystem II core complex and the peripheral antenna [de Weerd et al., 2002].

The first part (PS II core complex) contains the photochemical reaction centre (known as P680) bound to D1 and D2 proteins. Also contained in this section are the two sequence-related light-harvesting complexes CP43 and CP47. These complexes each bind ~14-16 Chlorophyll a (Chl a) and ~2- 3 β - carotene molecules [de Weerd et al., 2002].

The second part (peripheral antenna complex) of PS II is formed by the peripheral antenna, which consists of a number of pigment-protein complexes of the Cab gene family (e.g. CP24, CP26, CP29 and LHC II in green plants), all binding several Chl a, Chl b, and xanthophylls molecules. Some of these peripheral antenna molecules are closely associated with the PSII core complex forming what is known as PS II – LHC II super complex [de Weerd et al., 2002], see Figure 2.9 below:

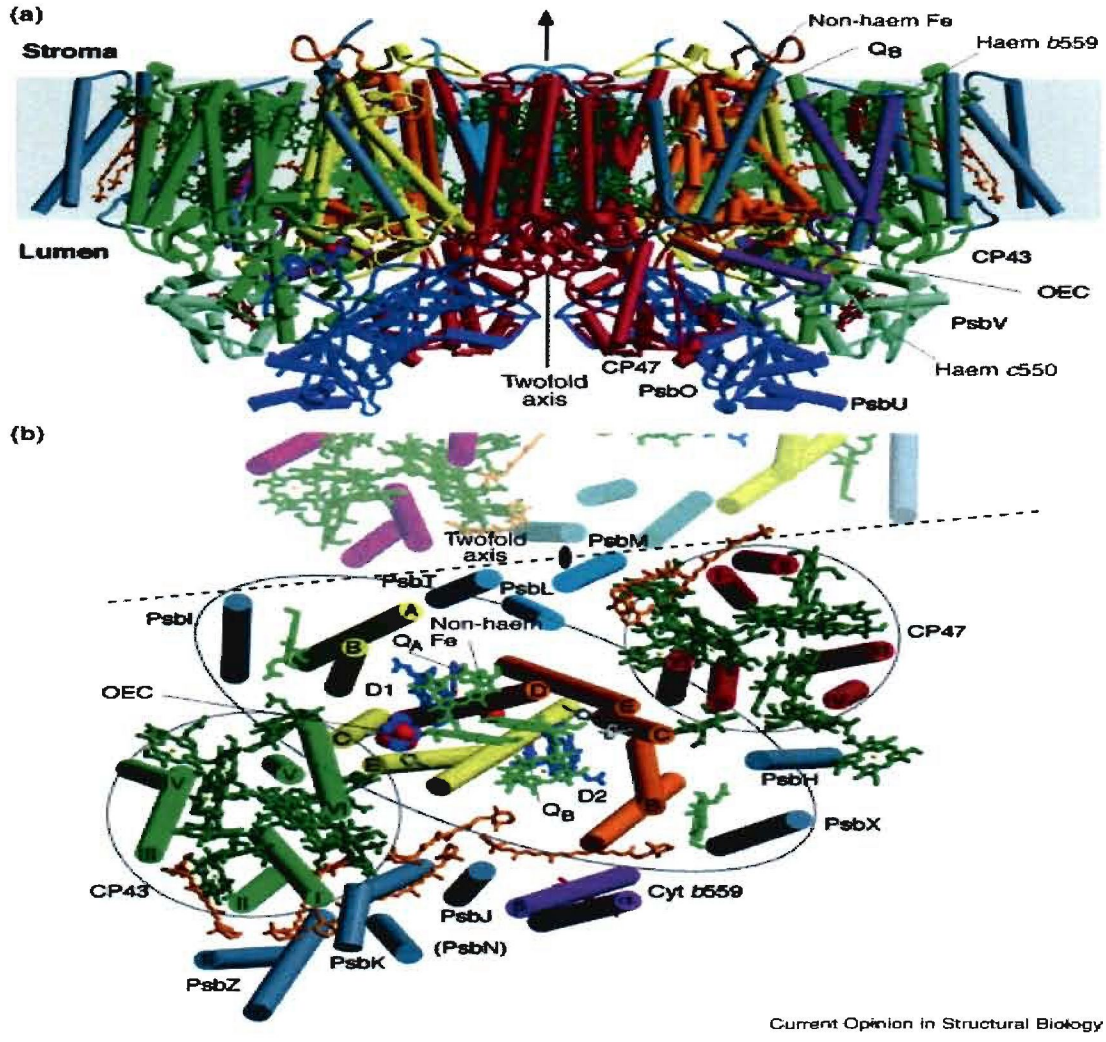

Figure 2.9: Overall structure of PS II from cyanobacterium T*hermosynechococcus enlongatus* at 3.5 Å resolution, **(a)** View of the PS II dimer perpendicular to the membrane normal, **(b)** View of the PS II monomer along the membrane normal from the lumenal side [Iwata & Barber, 2004]

2.3.1.1 Photosystem II associated complexes: LHC II

Light harvesting complex II (LHC II) is the major component of PS II. In higher plants, it binds chlorophyll a, b as well as xanthophylls. LHCII is a trimeric membrane protein in its native form, and chemical analysis has revealed that each monomer binds two types of chlorophylls, 8 Chl *a* and 6 Chl *b* and four types of carotenoids, 2 luteins (Lut), 1 neoxanthin (Neo), and 0.3 violaxanthin (Vio) [(Liu et al, 2004), (Peterman et al., 1997), (Croce et al., 1999)]. It accounts for approximately half of the total chlorophyll as well as the total protein in the membrane and has a chlorophyll a/b ratio of ~1:1[Allen and Staehelin, 1992].

It is one of the few membrane proteins with well characterised crystallographic structure (2.72 Å resolution), and in the past decade its polypeptide chain, pigment composition and lipid content have been investigated in depth [(Liu et al., 2004), (Simidjiev et al., 1997)].

LHC II plays various essential roles that include the following [Simidjiev et al., 1997]:

- Harvesting solar energy (light) and transferring the excitation energy to a reaction centre as a primary role.
- It plays an important role in mediating the stacking of thylakoid membranes.
- It participates in different regulatory photo-physical processes in the antenna complex.
- LHC II has been shown to play an important role in the assembly of chirally organised macro-domains of PSII, a mechanism held responsible for the spatial separation of the two photosystems.

In this project, the focus was on LHCII, mainly because it is well characterised and understood, hence a good starting point for the goal of developing artificial systems.

2.3.2 Overview of photosystem I

Photosystem I (PSI) is commonly known as a pigment-protein complex embedded in thylakoid membranes together with PS II. It can photo-reduce ferredoxin (fd) by means of electrons from PSII fed through plastocyanin (PC) [Hiyama, 1996], and for this reason it can also be referred to as a "light-driven plastocyanin: ferredoxin oxidoreductase" although in the enzymological sense, the word "oxidoreductase" might not fit well because of its inherently irreversible nature.

The PSI core complex is a heterodimer of two polypeptides (PsaA and PsaB) 80 kDa in size. It binds a P700 (the photochemical reaction centre pigment: a heterodimer of chlorophylls a and a'), two phylloquinones, an iron-sulphur cluster and a number of light-harvesting chlorophyll a molecules. Thus far, approximately 15 other subunits (smaller than 20kDa) have been proposed to be members of the PSI complex [Carpentier, 2004].

Since the 1960s, efforts have been made to isolate PS I in a form of a complex, and currently a variety of preparations have been reported from numerous plants like spinach, peas and sugar beet. Their subunits compositions vary widely even within the same plant and the complexes are categorised into three types: Type I, II and III [Hiyama, 1996].

Type II is one of the most common types of PSI complexes and it consists of PsaA, PsaB, PsaC, PsaD, PsaE and very seldom a few other small polypeptides [Carpentier, 2004]. Photochemically active reaction centre particles (Type III) are core complexes that consist of only large subunits (PsaA and PsaB).

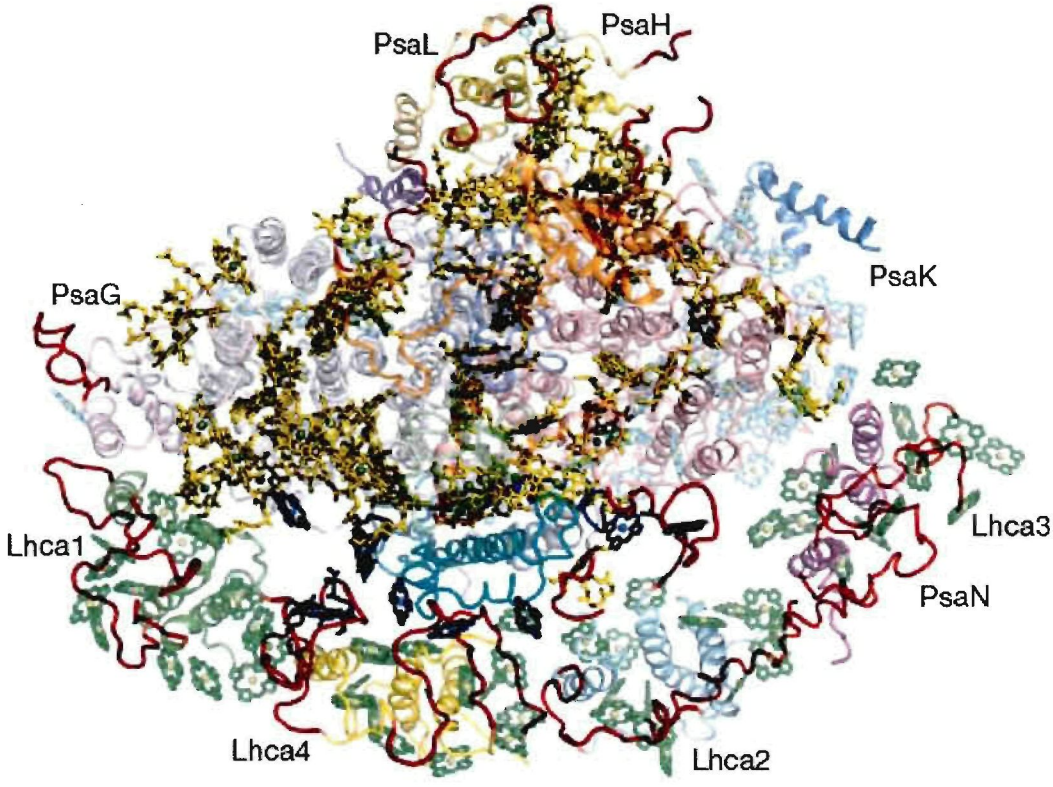

Figure 2.10: The structural model of plant photosystem I at 3.4 Å resolution, (view from the stroma). Novel structural elements that are not present in the previous model are shown as red ribbon structures [Amunts et al., 2007]

Figure 2.10 above shows the model of plant photosystem I at 3.4 Å. Chlorophylls with detected phytyl side chains, revealing that the orientation of the Qx and Qy transition dipole moments, are yellow. The rest of the reaction centre chlorophylls are cyan; gap chlorophylls are blue and chlorophylls of LHCI are green. The positions of PsaG, H, K, L and N, as well as the various LHCI monomers, are indicated. Each individual subunit is coloured differently [Amunts et al., 2007].

2.3.3 The reaction centre

Photosynthetic reaction centres are membranespanning complexes of polypeptide chains and cofactors that catalyse the first steps in the conversion of light energy to chemical energy during photosynthesis. The reaction centres of photosynthetic purple bacteria consist of at least three protein subunits; the L (light), M (medium) and H (heavy) subunits, and in some species, the fourhaem cytochrome c is the fourth and the largest subunit. The L and M subunits bind bacteriochlorophylls (BChl).

The central part of the RC is formed by the closely associated subunits L and M form. The L and M subunits (mainly α) share the same fold; the most prominent structural features of each of these subunits are five transmembrane helices. Both the polypeptide backbone of the L and M subunits and the attached prosthetic groups, show a high degree of local twofold symmetry, with the symmetry axis perpendicular to the membrane plane. On either side of the membranespanning region, the L-M complex is a flat surface parallel to the membrane plane [Blankenship, 1996].

There are three distinct segments in the H subunit; the N terminal segment, beginning from formylMet, containing the only transmembrane helix of subunit H, a surface segment, which is mostly in contact with the cytoplasmic side of the L-M complex; and a globular segment consisting mainly of ß sheets. In *Rps. viridis*, the cytochrome subunit binds at the periplasmic side of the L-M complex. Neither the H subunit nor the cytochrome obeys the local symmetry possessed by the L-M complex; the cytochrome has internal local symmetry of its own [Blankenship, 1996].

Except the carotenoid, prosthetic groups in the L-M complex are arranged into two approximately symmetric branches, known as the A branch and the B branch, each consisting of two BChl, one BPh and one quinone. In the nomenclature suggested by Deisenhofer and Michel (1992), D is used for the special pair of closely associated BChl, B for the accessory BChl, Φ for the BPh and Q for the quinone. The branches are denoted by subscripts A and B; since D belongs to both branches, its two BChl are denoted by subscripts L and M according to the subunit to which their Mg^{2+} is linked [Blankenship & Parson, 1979].

Two His residues each from the subunits L and M are the fifth ligands of the Mg^{2+} of the BChl. The special pair D_L-D_M is located near the periplasmic membrane surface on the symmetry axis. The A and B branches lead through the membrane to the cytoplasmic site. The high spin iron is bound near the cytoplasmic membrane surface, between the quinones close to the symmetry axis, and is bound to four His and one chelating (τ^2) Glu. These iron metals can be removed [Blankenship & Parson, 1979], or exchanged with several divalent metals [Debus et al. (1986)] without impairing the function of the RC.

The carotenoid is associated with the BChl of the B branch. Its possible function is to protect the RC by quenching the triplet state of D before it can sensitise the formation of an oxygen radical, a powerful oxidising agent [Frank, 1993]. Crystallographic and spectroscopic data show that the carotenoid molecule is not in an all *trans* conformation but has a single *cis* bond near the centre of the polyene chain [Frank, 1993], see Figure 2.10 below.

In purple bacterium *Acididphilium rubrum*, the RC contains a BChla containing Zn as a central metal and Bacteriopheophytin a (BPh a) [Tomi et al., (2007)].

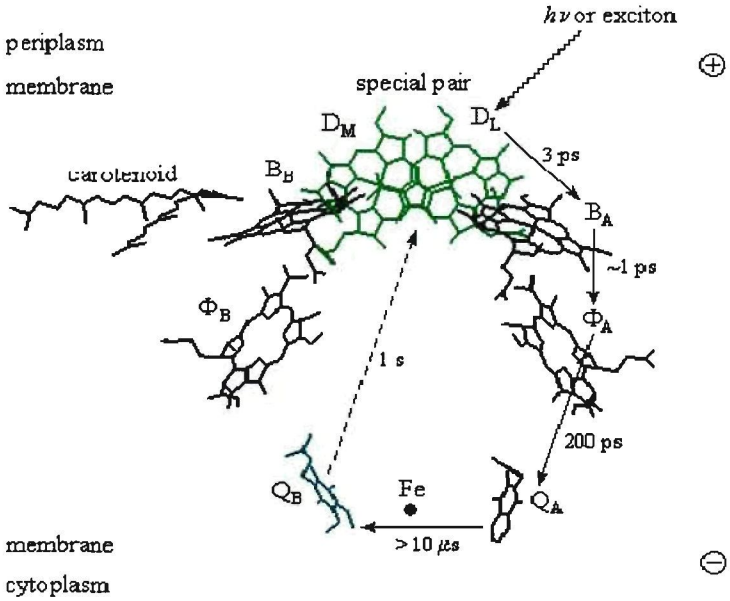

Figure 2.11: Arrangement of the special pair, accessory pigments and irons in the reaction centre illustrating excitation pathway [Farabee, 2006]

Figure 2.12 below serves as a comparison graph between the bacterial reaction centre and plant reaction centre to illustrate the similarities between the two reaction centres. The first part illustrates the bacterial reaction centre. The L and M subunits, which bind the pigments active in charge separation (red), are related by local near two-fold symmetry. The reaction centre is surrounded by a ring of light-harvesting proteins (LH1). Electrons are fed into the reaction centre by a haem-binding cytochrome (cyt) [Rhee et al., 1998].

The second part illustrates photosystem II. The D1 and D2 proteins are structurally and functionally homologous to the L and M subunits of the bacterial reaction centre and hold the active pigments in a similar configuration. Light energy is collected by LHCII and channelled into the reaction centre by the core antenna proteins, CP43 and CP47, which are positioned at either side of the D1-D2 hetero-dimer [Rhee et al., 1998]. The resulting charge separation enables the manganese cluster on the luminal surface to withdraw electrons from water, releasing oxygen into the atmosphere.

The third part is photosystem I. The PsaA and PsaB proteins form a PSII-like hetero-dimer. PsaA and PsaB each consist of a reaction centre system equivalent to D1 or D2, and a core antenna equivalent to CP43 or CP47. Electrons are taken from reversibly bound plastocyanin (PC) on the luminal side, and delivered to the iron sulphur clusters (FeS) on the stromal side, where they are used to reduce NADP+ to NADPH [Rhee et al., 1998].

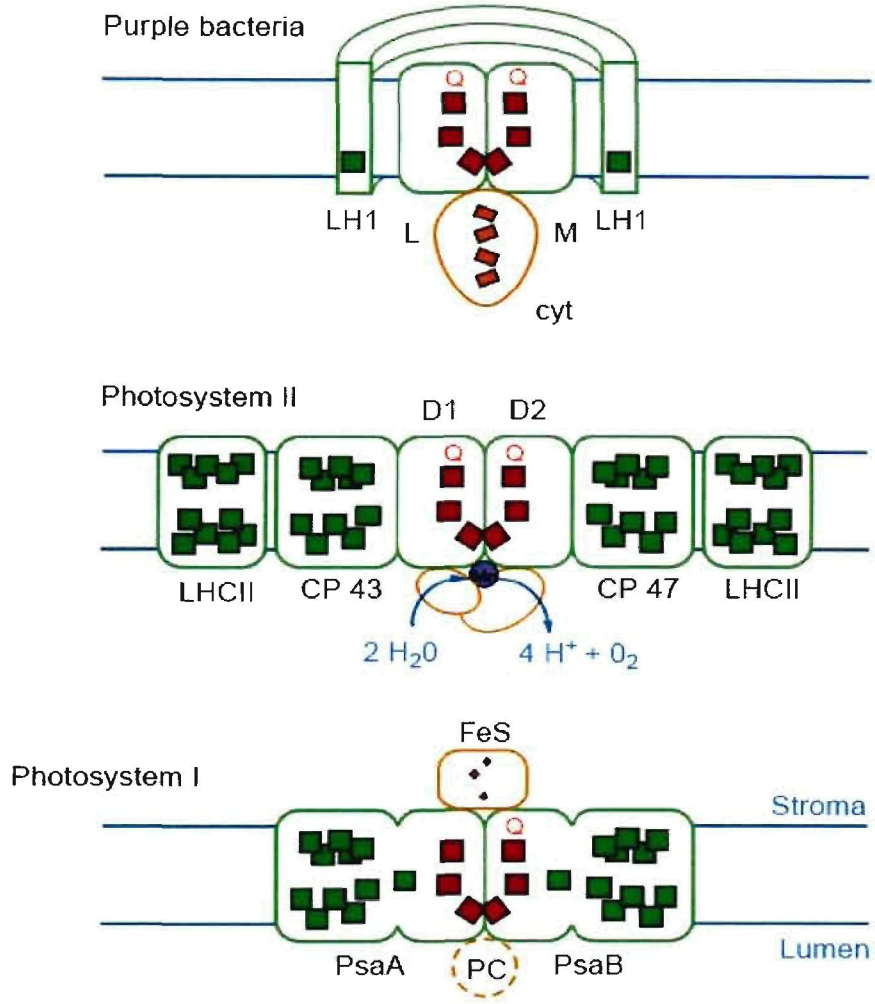

Figure 2.12: Comparison of the three types of reaction centre found in photosynthetic organisms [Rhee et al., 1998]

2.4 Energy transfer from light harvesting complexes to the reaction centre

There are a number of mechanisms in which energy transfer processes can occur within a photosynthetic unit. The Förster mechanism operates over large distances, and depends upon the relative orientations of the pigments and the spectral overlap between the fluorescence band of the donor and the absorption band of the acceptor [Förster, 1948].

The excitation energy can be transferred by resonance energy transfer to a neighbouring molecule if their energy level difference corresponds to the quantum of the excitation energy. In this process, the excitation energy is transferred, promoting an e^- in the receptor molecule to a higher excited energy state as the photo-excited e^- in the original absorbing molecule returns to its ground state. This is called the Förster resonance energy transfer whereby quanta of light falling anywhere within an array of pigment molecules can be transferred ultimately to a specific photochemical reactive site [Garrett & Grisham, 1999].

Other mechanisms include those proposed by many researchers; In 1953, Dexter pointed out that there existed another mechanism for excitation transfer, which is based on electron exchange between the donor D and the acceptor A (Dexter 1953), and which has been described in detail for light harvesting in purple bacteria by Damjanovic et al. [1999].

These two mechanisms mentioned above are commonly known as the Coulomb (Förster mechanism in its generalised form) and exchange mechanisms for excitation transfer that differ significantly in their operative range. While the Coulomb mechanism is effective over distances of typically 20–50 Å, the exchange mechanism is effective only when there is sufficient overlap of the wave functions of D^* and A, i.e., for distances of a few Å [(Dexter 1953), (Damjanovic et al., 1999)].

In recent years, the advent of ultra-short pulsed laser systems (ultra-fast pump probe transient absorption spectroscopic techniques) has greatly enhanced the study of photosynthetic energy transfer processes; see Chapter 3.1 [(Gradinaru et al., 2001, Groot et al., 2004, Doust et al., 2005)]. Using such pulsed light sources enables the pigments to be excited in unison with a monochromatic light source. This excites the pigments at a pre-set temporal origin within the pulse duration (Mančal et al., 2008). This coupled to theoretical modelling is beginning to provide evidence that quantum coherence plays a role in making the energy transfer process highly efficient. However, the exact mechanism is still unknown (Lee et al., 2007).

2.4.1 Summary for energy migration

The light harvesting and energy transfer processes are initiated by the absorption of a photon by an antenna molecule, which occurs in about a femtosecond (1 fs = 10^{-15} s) and causes a transition from the electronic ground state to an excited state. Within 10^{-13} s, the excited state decays by vibrational relaxation to the first excited singlet state. The fate of the excited state energy is guided by the structure of the protein. Because of the proximity of other antenna molecules with the same or similar energy states, the excited state energy has a high probability of being transferred by resonance energy transfer to a near neighbour antenna molecule.

Exciton energy transfer between antenna molecules is due to the interaction of the transition dipole moment of the molecules. The probability of transfer is dependent on the distance between the transition dipoles of the donor and acceptor molecules, the relative orientation of the transition dipoles, and the overlap of the emission spectrum of the donor molecule with the absorption spectrum of the acceptor molecule. Photosynthetic antenna systems are very efficient at this transfer process. Under optimum conditions over 90% of the absorbed quanta are transferred within a few hundred picoseconds from the antenna system to the reaction centre which acts as a sink for the exciton energy [van Grondelle & Amesz, 1986].

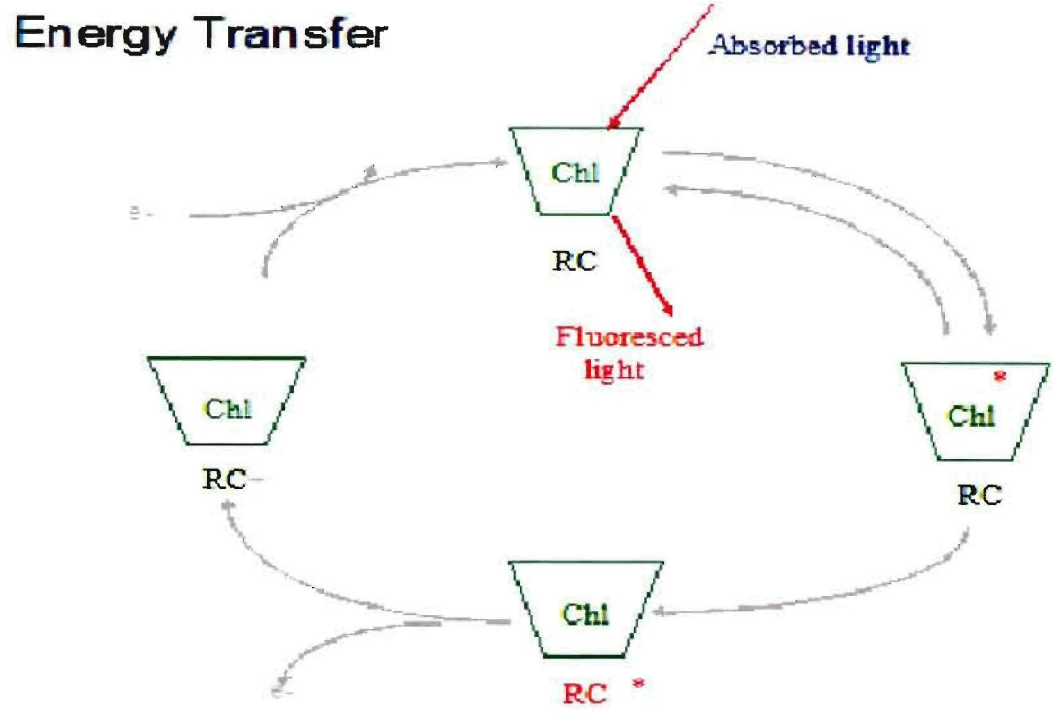

Figure 2.13: Illustrating a summary of energy transfer processes

2.4.2 Energy dissipation

If the reaction centres are "closed", exciton energy is not trapped and is dissipated as fluorescence or other modes of energy loss, mentioned in Section 2.2.1. The fluorescence lifetime of antenna BChl is in the order of 10 to 80 ps (what appears as fluorescence emission is mostly the energy that was not used for charge separation in the reaction centre). The fate of created excitons depends on the turnover rate of reaction centres and the number of excited states relative to the antenna molecules. Furthermore, the size of the photosynthetic unit (the number of antenna molecules per RC) and the topography of the photosynthetic units, seem to be important in determining the efficiency of energy transfer [Drews, 1985]. Figure 2.14 below shows the proposed excitation transfer pathway in bacterial photosynthetic unit.

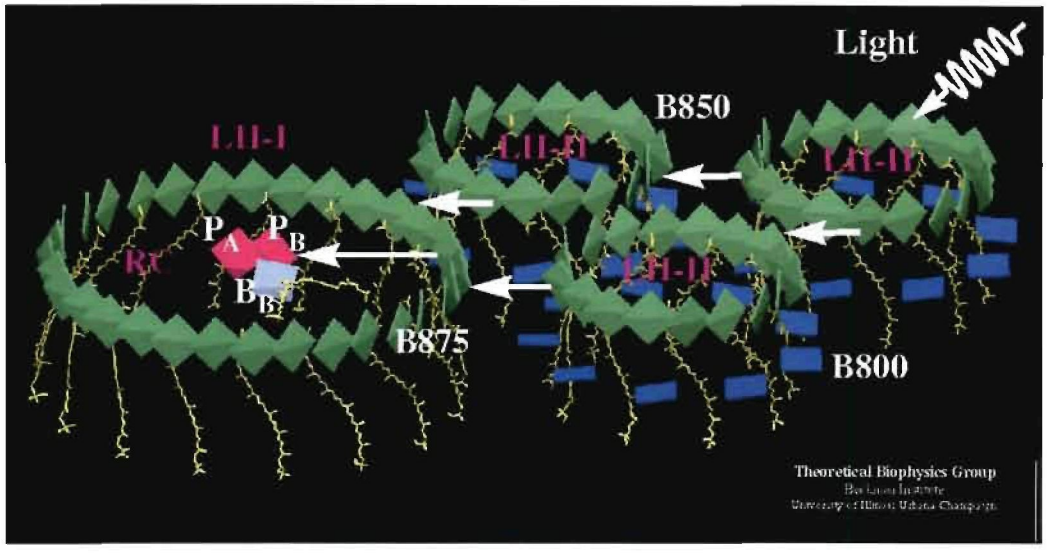

Figure 2.14: Excitation transfer in the bacterial photosynthetic unit [Humphrey et al., 1996]

The calculated time constants of 3.3 and 65 ps for the excitation transfer processes LH-II → LH-I and LH-I → RC in *Rb. sphaeroides* , respectively, are in agreement with experimental values of 3-5 ps and 35 ps [Damjanovic et al.,2000]. The time constant of ~1.33 and ~ 24.55 for the excitation transfer processes at 678 nm in higher plants have been observed by many researchers [de Weert et al., 2002].

van Grondelle and Amesz (1986), showed that it takes about 1 femtosecond (10^{-15} s) for a photon of light to be absorbed by an antenna molecule during the initiation of light harvesting reactions and taken to the excited state, within a picosecond (10^{-12}s), the excited state decays by vibrational relaxation to the first excited singlet state, and then the relaxation back to the ground state has a longer time decay.

When the exciton energy gets trapped by the reaction centre and redox reactions proceed, what is known as the light reactions of photosynthesis occurs. The following information is based on the reactions in higher photosynthetic plants.

2.5 Light reactions of photosynthesis

2.5.1 Photosystems I and II

This part of photosynthesis is divided into two phases or systems, called photosystem II (PS II) and photosystem I (PS I). Photosystems are arrangements of chlorophyll and other pigments occupying the thylakoids. Many prokaryotes have one photosystem (photosystem II), so named because it was the second photosystem discovered, but likely the first one evolved. Eukaryotes have both photosystems I and II. Photosystem I uses chlorophyll a referred to as P700, while photosystem II uses P680 as reaction centre pigments [Bailey, 2006].

Photosystem I provide the reducing power in the form of NADPH, while photosystem II splits water, producing molecular oxygen and feeds the electrons released during this process, into an electron transport chain that couples PSII to PSI. Photosystems I and II are linked via an electron transport chain so that the weak reductant generated by PS II can provide an electron to reduce the weak oxidant side of P700. Electron transfer between PS II and PS I pumps protons for chemiosmotic ATP synthesis [Garrett & Grisham, 1999].

Equation 2.5.1 below shows that light reactions of photosynthesis involves the reduction of $NADP^+$ using the electrons derived from water and activated by light, hv. ATP is generated in the process [Garrett & Grisham, 1999].

$$2H_2O + 2NADP^+ + x\ ADP + x\ Pi \xrightarrow[nhv]{} O_2 + 2NADPH + 2H^+ + x\ ATP + xH_2O$$

(Eqn: 2.5.1)

Where nhv = light energy

n = number of photons

h = Planck's constant

v =frequency of light.

Light energy is necessary to make the unfavourable reduction of $NADP^+$ by H_2O (where its standard reduction potential is -1.136 V and the Gibbs free energy is +219KJ/mol $NADP^+$) thermodynamically favourable. The standard reduction potential for $NADP^+$/NADPH couple is -0.32 V, thus a strong reductant with the reduction potential more negative than -0.32V is required to reduce $NADP^+$ under standard conditions, and by similar reasons, a very strong oxidant will be required to oxidise water to oxygen [Garrett & Grisham, 1999].

2.5.2 Electron flow between photosystems II and I

The electron flow mechanisms described below was taken from a biochemistry textbook [Garrett & Grisham, 1999]. The flow of electrons between H_2O and P680 involves a specific protein tyrosine residue named D, which mediates electrons from water via the manganese (Mn) complex to $P680^+$. The oxidised form of D is a tyrosyl free radical species, D^+. The cycle begins when the exciton energy excites P680 to P680* (excited state of P680), and then this molecule donates an electron to a special molecule of pheophytin (Pheo). In Pheophytin the centrally coordinated magnesium $(Mg)^{2+}$ ion in chlorophyll a is replaced by $2H^+$. For an illustration of this electron transfer, see Figure 2.3.

After donating an electron, P680* becomes $P680^+$, an electron acceptor for D. From here electrons flow from pheophytin and specialised molecules of plastoquinone (Q) to a pool of plastoquinone within the membrane. Plastoquinone is mobile within the membrane because of its lipid nature, and therefore serves to shuttle electrons from PS II supra-molecule complex to the cytochrome b_6/cytochrome f complex. Alternate oxidation-reduction of plastoquinone to its hydroquinone form involves the uptake of protons. The asymmetry of the thylakoid membrane is designated to exploit this proton uptake and release so that protons accumulate within the thylakoid vesicle, establishing an electrochemical gradient necessary for ATP production.

From the cytochrome complex, the electrons go to the next acceptor, plastocyanin (PC), which is capable of migrating in and out of the membrane hence suited for shuttling electrons between the cytochrome b_6/cytochrome f complex and PS I.

When P700 is excited by light and oxidised by transferring its electrons to an adjacent chlorophyll a molecule (acceptor which is designated as A_0), $P700^+$ is formed, which readily gains an electron from plastocyanin. A_0 rapidly passes the electron to a specialised quinone molecule (A_1), which in turn passes the electron to the membrane bound ferredoxins (Fd). This Fd series ends with a soluble form of ferredoxin, Fds, which serves as the immediate electron donor to the flavoprotein (Fp) that catalyses $NADP^+$ reduction, namely Ferredoxin: $NADP^+$ reductase.

When the individual redox components of PS I and PS II are arranged as an electron transport chain according to their standard reduction potentials, the zigzag result resembles the letter Z laid sideways. See Figure 2.15 below.

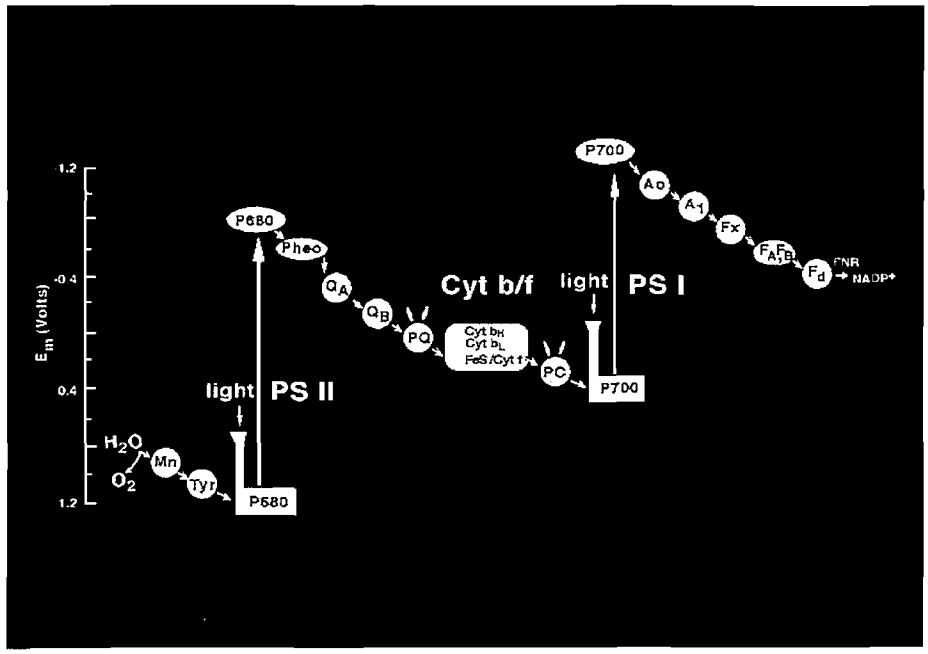

Figure 2.15: The Z scheme of photosynthesis representing a photosynthetic electron flow from H_2O to $NADP^+$.

CHAPTER 3

Background to characterisation methods

3.1 Ultrafast laser spectroscopy

Light-induced processes in living organisms, like the energy transfer in the early stages of photosynthesis, take place in extremely short periods of time, from a few femtoseconds (fs) to many nanoseconds [van Grondelle & Amesz, 1986]. In theory, the only tool that can be used to study these processes, is light itself, but over recent years, special tools have been developed to follow these processes [Vengris, 2005].

The ultrafast titanium: sapphire lasers that are now commercially available, allow for the generation of intense laser pulses with the duration of several tens of femtoseconds. These pulses can be used to build a 'camera' that can be able to follow the photoreactions of life. Ultrafast laser spectroscopy is the scientific and technological field that focuses on the application of lasers to study the ultrafast biological, physical and chemical processes.

3.1.1 Pump-probe

The most widely used variation of the ultrafast spectroscopy is pump-probe spectroscopy, which is also known as transient absorption spectroscopy. This technique uses a very simple concept that involves two short laser pulses: an intense pulse called the pump pulse, which induces or initiates a photoreaction in the system of interest, and a second weaker pulse called the probe, which monitors the corresponding change in the absorption spectrum (colour) of the sample.

Delay time can be introduced between these two pulses by mechanically delaying the probe pulse (changing the distance it has to travel) with respect to the pump pulse, and hence the corresponding absorption change in the sample of interest can be recorded at different time intervals after the arrival of the excitation pulse [Vengris, 2005].

Figure 3.1 below illustrates a typical pump probe setup (this specific setup is used at the National Laser Centre) to realise a condition where the pump and the probe pulses are overlapped in the sample and the probe pulse is then projected onto the detector. The components of the setup below allow one to obtain the light colours necessary for the experiments to be conducted [Vengris, 2005]. More details about the pump probe setup are provided in Chapter 4.5.

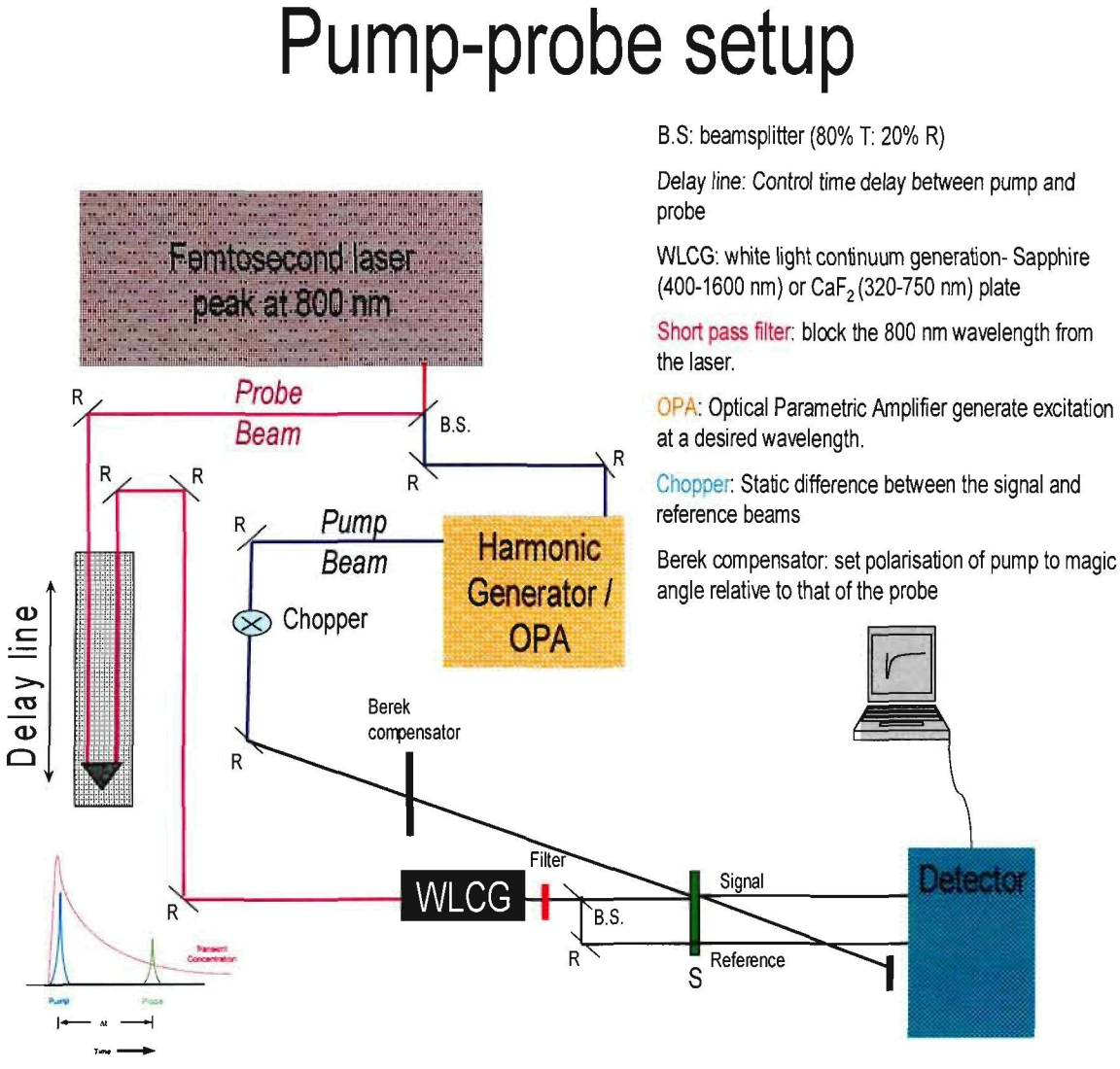

Figure 3.1: Set up for the pump probe experiment [Vengris, 2005]

The absorption spectrum of the sample has to be matched by the excitation (pump) pulse, while the probe pulse has to be able to monitor the absorption change at different wavelengths. Tuneable (525nm to 20μm) excitation pulses are obtained by using optical parametric amplifiers, where each photon of the incoming laser light is divided into two photons of varying energies. The distribution of the energy between these two photons depends on the spatial orientation or temperature of the non-linear crystal and the medium where the parametric amplification occurs [Vengris, 2005].

Most commercial lasers deliver near transform limited pulses i.e. where the spectral width of the pulse is dictated by its duration according to the Fourier transform, the spectrum of the probe pulse is artificially broadened by focusing it onto a non-linear material (sapphire in our specific case). When focusing ultrafast laser pulses of high power density into the media, the third-order nonlinear optical effect will induce a transient refractive index change in the media, giving rise to a transient change in the phase of the laser pulse propagating in the media in response. This effect is known as self-phase modulation [Dong-Hui, 2003].

Via this process of self-phase modulation, the spectrum of the laser pulse broadens to cover the whole of the visible range. This femtosecond 'white light' pulse is overlapped with the pump pulse from the optical parametric amplifier in the sample and then dispersed onto a multi-channel detector like a CCD (charge-coupled device) camera or an array of photodiodes, to enable one to measure the entire absorption spectrum of a sample at a specific delay time [Vengris, 2005].

3.1.2. Interpretation of the data obtained from pump-probe

Figure 3.1 above illustrates that the photo-induced spectrum of a sample of interest is dependent on the delay time between the pump and the probe pulse and hence it is measured. This dependency is often represented in the form of time-resolved difference spectrum, $\Delta A = \Delta A\ (t, \lambda)$, where ΔA represents the difference in absorption between the sample with and without the pulse. If a molecule within the sample absorbs a photon and goes to an excited state, there will be a decrease in absorption, i.e. a negative ΔA at wavelengths where that molecule absorbs in the ground state, as a result of most molecules being absent in that ground state [Vengris, 2005].

Molecules in the excited state can absorb another photon from the probe pulse and go into an even higher excited state through a process of excited state absorption (ESA), or they can emit a photon with similar characteristics as the one from the probe pulse, and hence return to the ground state through the process of stimulated emission (SE) [Vengris, 2005].

Another process can also occur, which is known as the ground state bleaching (GSB), where a molecule in the excited state can go back to the ground state, while passing the energy it possessed onto the next available energy acceptor in case of some biological photoreactions [Vengris, 2005].

In the case of ESA, there is an increase in absorption, hence a positive ΔA is observed, while in the case of SE and GSB, there is a decrease in absorption hence a negative ΔA is observed [Vengris, 2005]. The SE spectrum is always red shifted due to the conservation of energy (photons possess lower energy) compared to the ground state absorption spectrum and because ESA bands depend on the excited state structure of a particular molecule, they can be at any wavelength compared to the ground state absorption [Vengris, 2005].

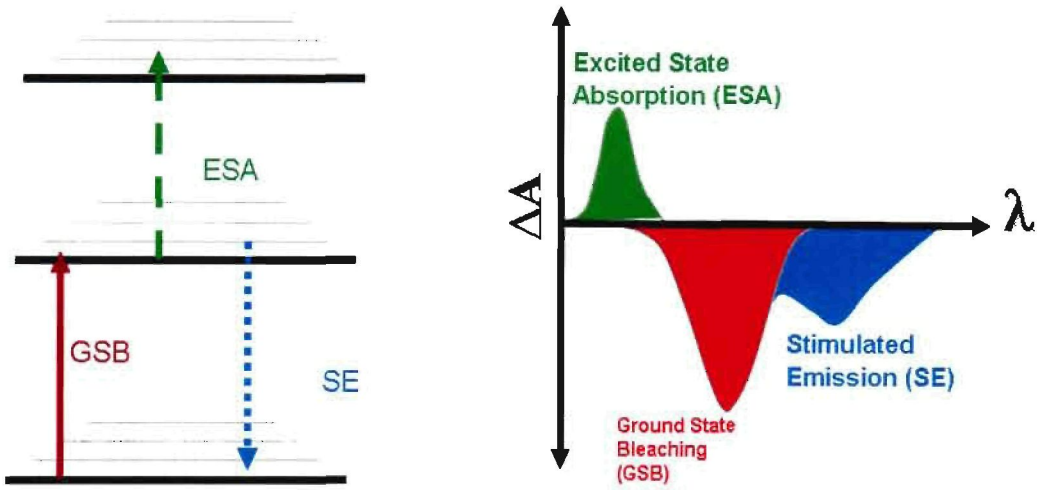

Figure 3.2(a): The energy level scheme of a molecule and the processes observed in pump probe experiments: ground state bleaching (GSB), stimulated emission (SE) and excited state absorption (ESA). **(b)** the contributions of different processes to the pump-probe spectrum [Vengris, 2005]

3.1.3 Technical specification of the NLC pump-probe set-up

Dr A du Plessis, Mr Saturnin and co-workers, performed all the characterisation work decribed below at the NLC. A sapphire plate (2.15 mm thick) was used to generate the white light continuum and Figure 3.3 below shows the spectrum of the generated white light continuum. The first spectrum (without filter) was recorded and a strong signal was observed around 795 nm, which is the signal from the fundamental of the Ti:sapphire femtosecond laser. To cut off this signal, a short pass filter was inserted in front of the spectrometer. A second spectrum (with filter) was recorded as indicated in Figure 3.4.

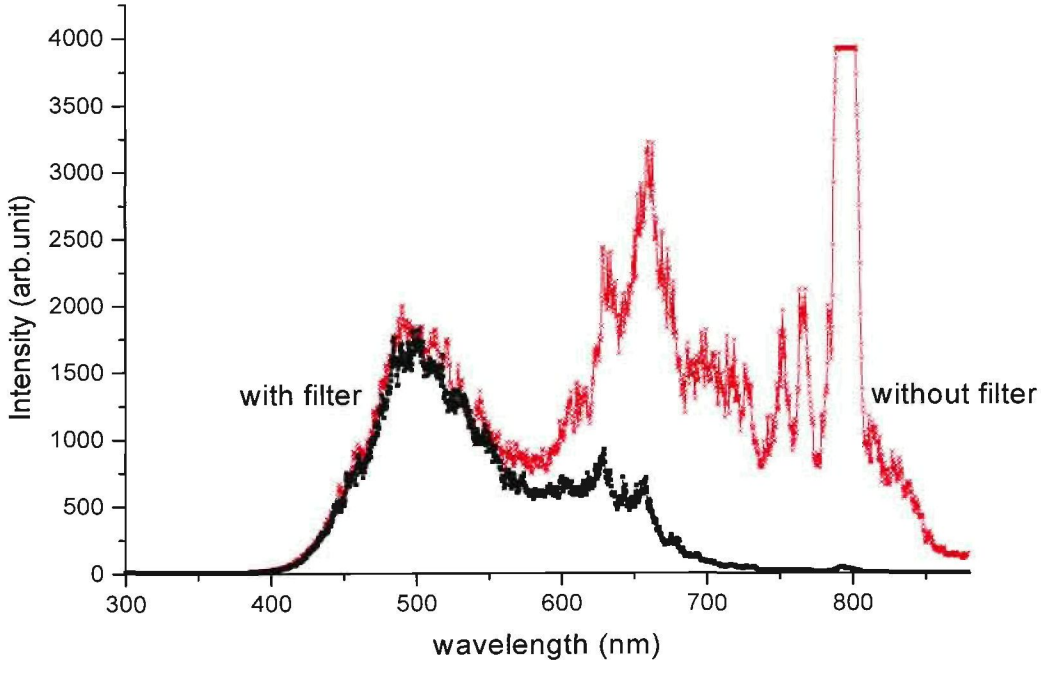

Figure 3.3: Spectra of the white light continuum used in the NLC pump probe system: with and without short-pass filter

The white light was then split (50%-50% beam splitter) into two parts: the probe and reference beams, respectively.

Malachite green dissolved in ethanol was used as a sample for this proof of principle experiment. A typical result of the transient absorption kinetics signal is shown in Figure 3.4 below. The figure illustrates the absorbance as a function of delay time at an absorbance wavelength of 610 nm. Since the OPA was also set to 610 nm (pump wavelength), this is called a one-colour pump probe measurement. The position of the strongest absorbance (0.045 arb. units) is relative to the position of the optical delay line. A fast decay process was observed after this point, which can be attributed to the excited state decay. A single exponential fit of the decay data indicates a time constant of 2.9 ± 0.1 ps.

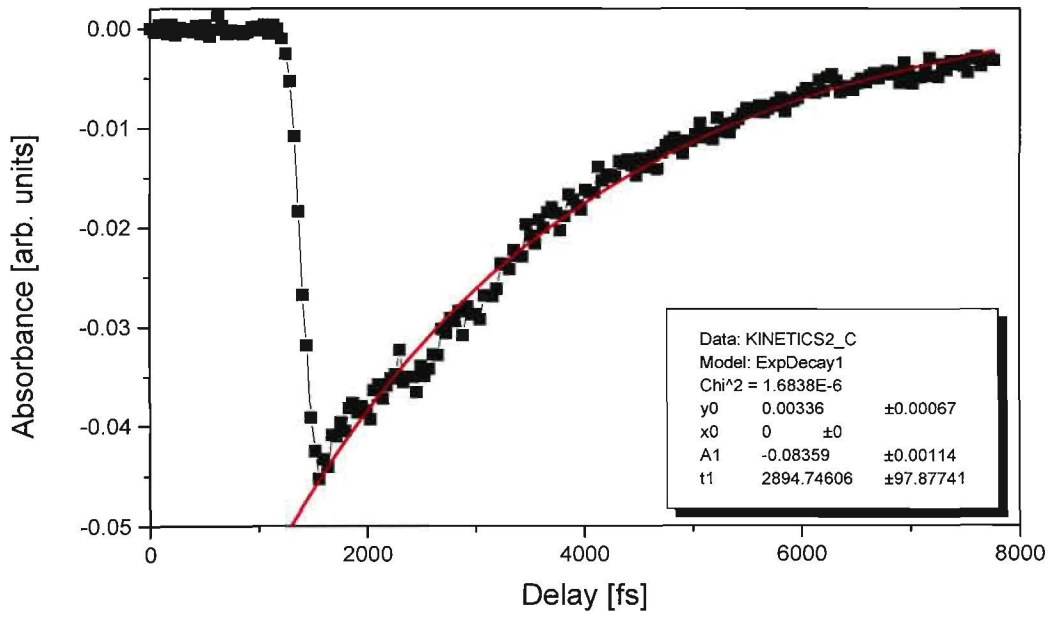

Figure 3.4: Absorbance at 610 nm as a function of delay time between pump and probe pulses in Malachite Green. In this case, the pump was set to 610 nm and the probe was a white light continuum

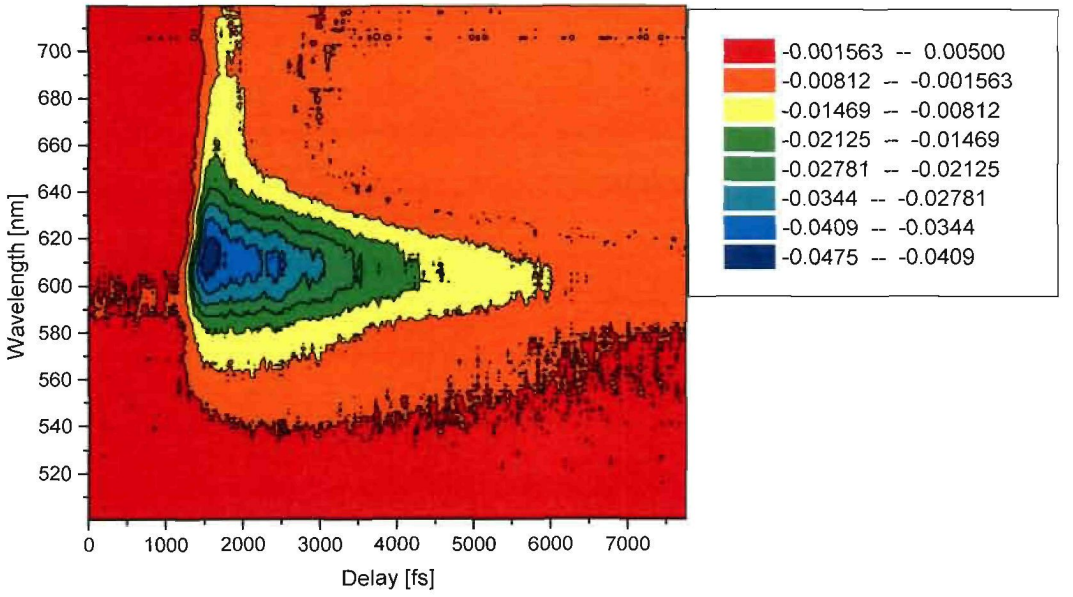

Figure 3.5: Transient absorption contour graph indicating measured absorbance spectra for a range of delay times between pump and probe pulses. The strongest absorbance occurs at 610 nm and at a relative delay of 1900 fs in this experiment

In Figure 3.5, a contour graph of the measured transient absorption of the Malachite green for the entire wavelength range 500 – 720 nm is shown. It can be seen in this figure that the strongest absorbance occurs at 610 nm and no other absorbance of interest occurs in this range, as expected.

3.2 Circular dichroism spectroscopy

Circular dichroism spectroscopy is a very powerful technique that yields secondary structural information of biological systems such as proteins [(Garab et al., 1987), (Barzda et al., 1994)]. This technique, together with many others, has been used for years to study and quantify optically active compounds and their interactions.

When light is passed through an absorbing optically active substance, the left and the right circularly polarised rays travel at different speeds, $c_L \neq c_R$, which leads to unequal wavelengths, and given these facts, the two rays are also absorbed at different extents ($\varepsilon_L \neq \varepsilon_R$). The difference $\Delta\varepsilon = \varepsilon_L - \varepsilon_R$ is known as Circular Dichroism (CD). In simple terms, CD is the difference in absorption between left and right- handed circularly polarised light [Barzda et al., 1994]. The difference in absorption for the two helical rays is recorded in all commercially available dichrographs. The equation below based on the Beer-Lambert-Bouguer Law, can be used to describe CD [Berova et al., 2000]:

$$\Delta\varepsilon = (1/cl)\, \Delta A \qquad \textbf{(Eqn: 3.2)}$$

Where A is the absorbancy $A = \log_{10} (I_0/I) = \varepsilon cl$, (the captured signal (A) is proportional to the concentration c and the pathlength l). I_0 is the intensity of the light impinging on the cell and I, is that when leaving. If c is given in moles per litre and l in centimetres, then ε is known as the molar absorption coefficient or molar absorptivity. For an optically active substance, the two absorptions (A) for the left and for the right circularly polarised light can be recorded, and on entrance into this substance, both the intensities I_{0L} and I_{0R} are equal, hence we leave the index L or R to obtain the equation above [Berova et al., 2000].

3.2.1 Circular dichroism effects

The CD effect arises because of certain asymmetries or chirality of the structure, which can either be intra- or intermolecular, as most if not all biological molecules (systems) are chiral [Barzda et al., 1994)]. The intrinsic CD of a small molecule, for a single electronic transition has the shape similar to that of absorption of the same molecule (with the sign determined by the handedness of the molecule) [Garab et al., 1987].

In molecular complexes or small aggregates, generally the CD is induced by short-range, excitonic coupling between chromophores. In macro-aggregates, chloroplasts and thylakoids, the CD signal is much stronger, with non-conservative, anomalously shaped bands accompanied by long tails outside the absorbance, and these have been attributed to long range chiral organisation of the chromophores [(Garab et al., 1987), (Barzda et al., 1994)].

3.2.2 Circular dichroism in light harvesting complex II

Light-harvesting Chl a/b pigment protein complex (LHCII) is one of the most abundant proteins in the biosphere, and its structure has been determined at 3.4Å resolution [Kuhlbrandt et al., 1994].

In this photosynthetic pigment- protein complex (LHCII):

- The chromophore's (chlorophyll's) density is high and the transition dipoles are coupled through energy transfer processes, which can extend to long distances [Barzda et al., 1994];

- The chlorophyll dipoles are aligned with respect to the protein axis and the macroaggregates sheet [(Garab et al., 1987), (Kiss et al., 1986)]; and

- In the macro-aggregates, the trimeric organisation and/ asymmetric adhesion of trimers may introduce long-range chirality [Butler & Kuhlbrandt., 1988].

Hence, three-dimensional aggregates of LHCII larger than one quarter of the wavelength of the incident light are expected to exhibit psi-type (polymerisation- or salt-induced) CD bands [Kim et al., 1986].

Psi-type aggregates are three-dimensional macro-aggregates containing a high density of chromophores that are interacting and possess sizes corresponding to a degree with the wavelength of the measuring light [Barzda et al., 1995]. LHCII trimers *in vitro* (isolated), also readily form large macro-aggregates with long-range chiral order, which can be recognised based on the presence of intense psi-type CD bands.

Long-range chirality is in turn essential for the long distance migration of energy [Simidjiev et al., 1997]. This characteristic of LHC II is essential for the purposes of this study, which is to prepare a LHCII sample that can undergo energy transfer, and this is evident when the CD spectrum of LHCII has an asymmetric band (psi-type CD band) at a wavelength of interest, which is 680nm for the purposes of this study.

3.2.3 CD signal intensity or amplitude

The intensity (amplitude) of the CD band in long-range chiral order is strongly dependent on the size of the aggregates [(Garab et al., 1991), (Barzda et al., 1994)]. Tightly stacked three-dimensional lamellar aggregates produce anomalous CD bands with psi-type CD features. The same psi-type bands with smaller amplitude are observed in loosely stacked lamellar aggregates. Aggregates that are not with well-defined structures have no intense psi-type CD bands. Unstacked, disordered lamellar aggregates also give CD bands that indicate that macro-aggregation does not interfere with the characteristic excitonic CD bands of the LHCII trimers (see Figure 3.6 below) [Simidjiev et al., 1997].

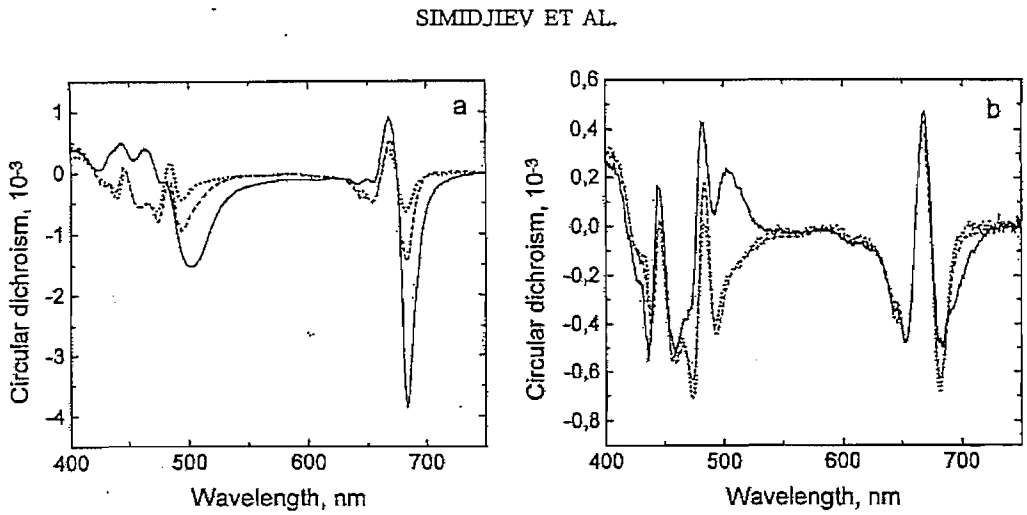

Figure 3.6: CD spectra of different types of LHCII aggregates. a) Tightly (-), and loosely (---) stacked lamellar aggregates, and disordered (...) macro-aggregates. B) Unstacked, disordered lamellar aggregates (-). [Simidjiev et al., 1997]

3.3 Gel electrophoresis

Gel electrophoresis is a technique that can be used to separate charged molecules such as proteins and DNA, according to their physical properties (size and charge) as they are moved through a gel by an electrical current. Proteins are commonly separated using polyacrylamide gel electrophoresis (PAGE). This technique is either used to characterise individual proteins in a complex sample or to examine multiple proteins within a single sample.

PAGE can be used as a preparative tool to obtain a pure protein sample, or as an analytical tool to provide information on the mass, charge, purity or presence of a protein. Several forms of PAGE exist and can provide different types of information about the protein(s). Non-denaturing PAGE, also called native PAGE, separates proteins according to their mass: charge ratio. SDS-PAGE, which is the most widely used electrophoresis technique, separates proteins primarily by mass. Two-dimensional PAGE (2-D PAGE) on the other hand, separates proteins by their isoelectric point (pI) in the first dimension and by mass in the second dimension [Lacks et al. 1979].

Acrylamide is the material of choice for preparing electrophoretic gels to separate proteins by size. Acrylamide mixed with bisacrylamide forms a cross-linked polymer network when the polymerising agent, ammonium persulfate (APS), is added (see Figure 3.7). APS produces free radicals much more rapidly in the presence of TEMED (N, N, N, N'-tetramethylenediamine). The size of the pores created in the gel is inversely related to the amount of acrylamide used. For example, a 7% polyacrylamide gel will have larger pores in the gel than a 12% polyacrylamide gel. Gels with a low percentage of acrylamide are typically used to resolve large proteins and high percentage gels are used to resolve small proteins [Lacks et al., 1979].

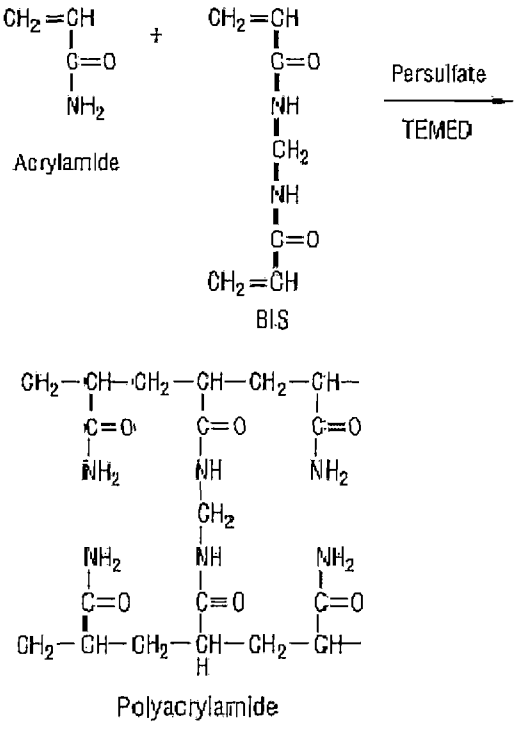

Figure 3.7: Polymerisation and cross-linking of acrylamide [Lacks et al., 1979]

3.3.1 Native PAGE

Because no denaturants (materials that will disrupt the structure of the protein) are present in native PAGE, subunit interactions within a multi-meric protein are generally retained and information may be gained about the quaternary structure of that particular protein. In addition, many proteins have been shown to be enzymatically active following separation by native PAGE. Thus, native PAGE may be used for the preparation of purified, active proteins [Rothe and Maurer, 1986].

Proteins may be recovered from a native gel by passive diffusion or electro-elution after performing native PAGE. In order to maintain the integrity of proteins during electrophoresis, it is important to keep the apparatus cool and to minimise the effects of denaturation and proteolysis.

Extremes of pH should generally be avoided in native PAGE, as they may lead to irreversible damage, such as denaturation or aggregation of the protein of concern [Bollag et al. 2002].

3.3.2 SDS-PAGE

In SDS-PAGE applications, the sample applied to the slab gel has been treated with the detergent sodium dodecyl sulfate (SDS). This ionic detergent denatures the proteins in the sample and binds tightly to the uncoiled molecule. The SDS molecules mask the intrinsic charge of the protein and create a relatively uniform negative charge distribution caused by the sulphate groups on SDS. When an electric current is applied, all proteins will move through the gel toward the anode, which is located at the bottom of the gel [Lacks et al., 1979].

The SDS-PAGE gel separates proteins primarily according to their size because the SDS-coated proteins have a uniform charge: mass ratio. Proteins with less mass travel more quickly through the gel than those with greater mass because of the sieving effect of the gel matrix. Protein molecular weights can be estimated by running standard proteins of known molecular weights in a separate lane (first lane) of the same gel [Rothe and Maurer, 1986].

To obtain optimal resolution of proteins, a "stacking" gel is poured over the top of the "resolving" gel. The stacking gel has a lower concentration of acrylamide (larger pore size), lower pH and a different ionic content. This allows the proteins in a lane to be concentrated into a tight band before entering the running or resolving gel and produces a gel with tighter or better-separated protein bands. The resolving gel may consist of a constant acrylamide concentration or a gradient of acrylamide concentration (high percentage of acrylamide at the bottom of the gel and low percentage at the top) [Bollag et al. 2002].

A gradient gel is prepared by mixing two different concentrations of acrylamide solution to form a gradient with decreasing concentrations of acrylamide. As the gradient forms, it is layered into a gel cassette. A gradient gel allows separation of a mixture of proteins with a greater molecular weight range than that of a fixed acrylamides concentration. If a sample contains proteins with large differences in molecular weights, then a gradient gel is recommended. A stacking gel is unnecessary when using a gradient gel since the continually decreasing pore size performs this function [Bollag et al. 2002].

3.3.4 Isoelectric focusing and two-dimensional gels

An isoelectric focusing gel (IEF gel) can be used to separate proteins according to their charge and to determine the pH at which a protein has a net charge of zero. This pH is known as the pI of the protein and is a distinguishing characteristic of the protein that provides useful information for purifying and handling of the protein. The pI of a protein is determined by the number of acidic and basic residues (e.g. amino acids) in the protein [Coligan et al., 2002].

At physiological pH, the carboxyl groups of acidic residues are predominantly deprotonated (lose electrons) and impart a negative charge. In contrast, the amine groups of basic residues are protonated (gain electrons) and carry a positive charge. By identifying the pI value of a protein, buffer systems for large-scale purification can be designed. For example, a protein with a pI of 5.6 will have a net charge of zero in a solution at pH 5.6. As the pH of the buffer system is increased, this protein (pI 5.6) takes on an overall negative charge because the carboxyl groups and amines are deprotonated [(Coligan et al., 2002), (Hames & Rickwood, 1990)].

The protein can then be purified on a DEAE ion exchange column in a buffer at pH 8.0. The negative charges will cause the protein to be retained on the positively-charged column. To perform IEF, a pH gradient is established in a tube or strip gel using a specially formulated buffer system or ampholyte mixture. Ampholytes are a mixture of amino acid polymers that have surface charges corresponding to different pH ranges and are available as immobilised pH gradient (IPG) strips for consistency and convenience [Hames & Rickwood, 1990)].

A protein sample is loaded onto the gel and electrodes are attached (anode at the acidic end of the gradient and cathode at the basic end of the gradient). Proteins with a net positive charge on the surface will migrate to the cathode when an electrical current is applied. Negatively charged proteins will move towards the anode. When the protein in the pH gradient reaches a zone in which the net surface charge is zero, it will no longer migrate. At this point the protein becomes "focused" and a band is formed in the gel [Coligan et al., 2002), (Hames & Rickwood, 1990)].

Following isoelectric focusing, a protein mixture may be separated in a second dimension by SDS-PAGE. This technique, known as 2-D PAGE, is used to resolve complex protein mixtures into the greatest number of individual protein "spots". The IEF gel is equilibrated with SDS and laid across the top of an SDS-PAGE gel. Current is applied and the proteins migrate into the gel where separation occurs according to mass [Coligan et al., 2002].

This two-dimensional separation of proteins according to pI and mass allows the resolution of proteins that would not normally be separated by a one-dimensional method. Several thousand protein spots may be resolved on a single 2-D PAGE gel, making this technique suitable for proteomics analysis [Coligan et al., 2002].

3.4 Thin-layer chromatography

Chromatography is used to separate mixtures of substances into their constituents. All forms of chromatography work on the same principle in a sense that they all have a stationary phase (a solid or a liquid supported on a solid) and a mobile phase (a liquid or a gas). The mobile phase migrates through the stationary phase while carrying the constituents of the mixture with it. Different constituents travel at different rates [IUPAC, 1993].

Thin-layer chromatography uses a thin, uniform layer of silica gel or alumina coated onto a piece of glass, metal or rigid plastic. The silica gel (or the alumina) is the stationary phase. The stationary phase for thin-layer chromatography also often contains a substance that fluoresces in UV light to make visualisation of the compounds contained in the mixture of interest possible when using UV light. The mobile phase is a suitable liquid solvent or mixture of solvents [Vogel et al., 2008].

A small amount of the mixture to be analysed is spotted near the bottom of the TLC plate (A pencil line is drawn 1 cm from the bottom of the plate). The plate is then placed in a shallow pool of a solvent in a developing chamber (TLC chamber) so that only the very bottom of the plate is in the liquid. This liquid, or the eluent, is the mobile phase, and it slowly rises up the TLC plate by capillary action [Stoddard, 2007].

While the solvent moves past the spot that was applied up the plate, equilibrium is established for each constituent of the mixture between the molecules of that constituent which is adsorbed on the solid and the molecules that are in solution. In principle, the constituents will differ in solubility and in the strength of their adsorption to the adsorbent and some constituents will be carried farther up the plate than others [Vogel et al., 2008].

When the solvent has reached the top of the plate, the plate is removed from the developing chamber, dried, and the separated constituents of the mixture are visualised. If the constituents are coloured, visualisation is easy and can be done with the naked eye. When the constituents are not coloured, a UV lamp is used to visualise the plates [Stoddard, 2007].

3.4.1 Extraction for thin layer chromatography

This technique was used to determine which pigments were present in the samples used during this study. Spinach leaves were used in this particular case as they photosynthesise, are easy to use when extracting light harvesting complexes, are well characterised and hence are a very good starting point when benchmarking a system like the pump probe system. They also contain pigments very important during the light harvesting processes of photosynthesis, such as chlorophylls and carotenes, and these were the pigments that were illustrated on the TLC plate [Rich et al. 2008].

These pigments are non-polar and will dissolve easily in non-polar organic solvent because of the "like dissolves like" rule. Acetone (non-polar organic solvent) was added into the extracted LHC II sample, and unfortunately, it dissolves almost anything including unwanted materials in the sample [Rich et al. 2008].

Chlorophylls and carotenes do not dissolve well in water, but they dissolve very well in hexane. Other materials in the extract above do not dissolve in hexane and only dissolve in water. Water and hexane do not mix because of the difference in their densities and hence form two layers. This allows for the separation of the chlorophylls and carotenes from the water-soluble compounds. After vigorous shaking to mix the two layers temporarily, time is given to allow the mixture to separate. The pigments will dissolve in the top hexane layer and all the unwanted materials will remain in the bottom water layer [Rich et al. 2008]. After this, the sample can then be loaded onto a TLC plate as described in Chapter 4, Section 4.4.4.

CHAPTER 4

Experimental procedure

4.1 Experimental procedures

LHC II was prepared from spinach leaves (with good turgor and dark green colour) as described before by Krupa et al. [1987], taken from the Photosynthetic Research Protocols by Carpentier [2004:274], with a few modifications to suit the experimental conditions. The leaves were grown at the green house within the Council for Scientific and Industrial Research (CSIR) Campus-Biosciences, and the entire experiment was performed under normal laboratory light and on ice.

The prepared samples (extracted LHCII) were stored in the dark at -87°C (in a Dairei freezer) for up to a month without the loss of their lamellar structure. Thawing and re-freezing can lead to complete degradation of these properties. The prepared sample was diluted in buffer C to obtain an absorbance of ~1 in a 1cm optical pathlength cuvette at 430nm and 680 nm for all characterisation methods as well as for the pump probe experiments.

Figure 4.1: Spinach leaves used for the extraction of LHCII

4.2 Materials

All buffers were kept in the refrigerator (4°C) and used within 1 month.

4.2.1 Buffers

1. Buffer A: 50 mM Hepes, pH 7.8 (with NaOH), 0.4 M sorbitol.
2. Buffer B: 20 mM Hepes, 5 mM EDTA, pH 7.8 (with NaOH), 50 mM sorbitol.
3. Buffer C: 20 mM Hepes, pH 7.8 (with NaOH).
4. Buffer D: 0.5 M sucrose cushion equilibrated with 20 mM Hepes, pH 7.8 (with NaOH).
5. Buffer E: 50 mM Hepes, pH 7.8 (with NaOH) and 100 mM sorbitol.

The first three buffers (A-C) were the most used, buffers D and E were used when attempting to get tightly stacked lamellar aggregates.

4.2.2 Stock solutions

1. 20% v:v Triton-X 100 (Fluka) buffered with 20 mM Hepes, pH 7.8 (with NaOH), can be stored at 4°C for up to two months in a dark brown bottle.
2. 2 M KCl.
3. 1 M $MgCl_2$

4.3 Methods

4.3.1 Isolation of LHCII

1. Approximately 400 g of spinach was washed with cold water and then chilled in distilled water, and homogenised with a mixer (blender) in 250 mL of buffer A (the amount of spinach can be adjusted depending on how much sample is required).

2. The homogenate was then filtered through four layers of unused muslin.

3. It was centrifuged (using a Beckman Coulter, Avanti J-30I centrifuge) at 5000g for 5 minutes.

4. The supernatant was discarded and the pellet suspended in buffer B. A medium sized brush was used for crude homogenisation of the pellet. All the material was finely homogenised, without visible big particles.

5. Sample was again centrifuged at 10,000g for 10 minutes and then the supernatant was discarded.

6. The pellet was then resuspended in cold buffer C, and then homogenised as above. Two samples were kept at this stage: sample A and sample B, A = with adjusted absorbance of ~ 1 in a 1cm cuvette and B = just enough buffer C was added to make a well homogenised sample without visible big particles.

7. Triton-X 100 (Fluka) was added, from the solution, to obtain the final concentration of 0.7-0.9%. This is required for loosely stacked lamellar aggregates of LHCII (Type II). To get LHCII micro-crystals (Type IV: tightly stacked lamellar aggregates), the final Triton concentration has to be 1.1-1.3%. Sample A = Type IV and sample B = Type II.

8. The sample mixture was then continuously stirred on ice for at least 45 minutes, until the visible clouds disappeared. (Continue stirring up to 60 minutes if clouds are present).

9. After that, the sample was centrifuged at 30,000g for 40 minutes. The insoluble material was sedimented, and the supernatant predominantly contained LHCII.

Most characterisation methods were carried out using the product sample B from step 9, although further steps were carried out to try to get LHCII aggregates using KCl and $MgCl_2$ stock solutions mainly on sample A (that did not seem to have any effective change on the results).

Sample B, which contained mostly LHC II (loosely stacked lamellae), was used over sample A, due to the difference in intensity of the signal, especially when performing the pump probe experiments (diluted sample A gave a weak signal compared to the concentrated sample B). For all the characterisation methods, the product sample B was used and diluted with buffer C to obtain optimal conditions for the specific characterisation method used, and all the dilution factors are stated for each method.

4.3.2 Chlorophyll quantification

The amount of chlorophyll was calculated each time a preparation was performed and the value below is for the sample used to perform other characterisation methods as well as the pump probe experiments, but for all the prepared samples, the chlorophyll quantity was very close to the given values. All the calculations were made before the detergent (triton x-100) was added.

- Add 50 μL sample, $10cm^3$ of 80% v:v acetone
- Filter
- Read absorbance at 665nm and 649nm.

The calculation method was based on [Arnon, 1949)] equations.

Chlorophyll a = $[(A_{665} \times 11.63) - (A_{649} \times 2.39)] \times 0.2$ mg/cm^3

Total chlorophyll = $[(A_{665} \times 6.4) + (A_{649} \times 17.72)] \times 0.2$ mg/cm^3

Chlorophyll b = Total chlorophyll - chlorophyll a

Chlorophyll a/b ratio was also calculated.

4.4 Experimental setup for characterisation methods

4.4.1 Absorption spectrum

The absorption spectrum of the prepared LHC II sample was measured using a UV-1650 PC UV-VIS spectrophotometer; the spectrum was also measured with a Chirascan simultaneously while measuring circular dichroism spectrum for comparison. All these measurements were performed at room temperature.

4.4.2 Circular dichroism measurements

Circular Dichroism (CD) spectrum of the prepared LHC II sample was measured at room temperature using the Chirascan Circular Dichroism Spectrometer (Applied Photophysics) shown below, and was presented in both the units of absorbance and milli-degrees (mdeg). The prepared sample was diluted with buffer C until the absorbance was ~ 1.1 at 430nm and 0.9 at 680nm in a 1cm optical pathlength cuvette.

Figure 4.2: Chirascan Circular Dichroism Spectrometer

4.4.3 SDS-PAGE

The experimental method below describes the buffers used and the steps followed to achieve a good SDS-PAGE gel. All the equipment used for the gel preparation is from Bio-Rad.

Buffers used:

5x sample buffer
10% w/v SDS
10mM Dithiothreitol or beta-mercapto-ethanol
20% v/v Glycerol
0.2M Tris-HCl, pH 6.8
0.05% w/v Bromophenolblue

1x Running buffer:

25mM Tris-HCl
200mM Glycine
0.1% w/v SDS

Staining solution

0.15% (w/v) bromophenol blue in destaining solution

Destaining solution

Acetic Acid: 500ml
Ethanol: 2000ml
H_2O: 2000ml

1x Running gel solution

After adding TEMED and APS, the gel polymerised fairly quickly, so these were not added until the gels were ready to pour.

Table 4.1: Ingredients to make up the resolving/running gel solution

	12%
H_2O	10.2 ml
1.5 M Tris-HCl, pH 8.8	7.5 ml
20% (w/v) SDS	0.15 ml
Acrylamide/Bis-acrylamide (30%/0.8% w/v)	12.0 ml
10% (w/v) ammonium persulfate (APS)	0.15 ml
TEMED	0.02 ml

Stacking gel solution (4% Acrylamide):

Table 4.2: Ingredients to make up the stacking gel solution

H_2O	3.075 ml
0.5 M Tris-HCl, pH 6.8	1.25 ml
20% (w/v) SDS	0.025 ml
Acrylamide/Bis-acrylamide (30%/0.8% w/v)	0.67 ml
10% (w/v) ammonium persulfate (APS)	0.025 ml
TEMED	0.005 ml

Pouring the gels:

A percentage acrylamide based on the molecular weight range of proteins wished to be separated was chosen to be 12%:

Table 4.3: The different acrylamide percentages for gels based on molecular weight range of proteins

% Gel	MW Range
7	50kDa-500 kDa
10	20 kDa -300 kDa
12	10 kDa -200 kDa
15	3 kDa -100 kDa

The ingredients needed for the chosen percentage were mixed and quickly poured into the gel casting form, some room was left for the stacking gel (~ 2 centimetres below the bottom of the comb), by inserting the comb into the dry form, and marking a region below the comb for the height of the stacker needed. Bubbles were removed if present, and then the top of the gel was layered with water.

The gel was allowed about 30 minutes to polymerise completely. If fresh ammonium persulphate is always used, the gel polymerises more quickly and reliably. The reagents for the stacking gel were mixed, but leaving out the APS and TEMED until ready to pour the gel.

When the running gel was polymerised, the water was removed completely. Polymerising reagents were mixed and the stacking gel was poured on top of the running gel. Combs were inserted trying not to get bubbles stuck underneath, and the gel was allowed another 30 minutes to one hour for complete polymerisation. At this stage, the gels were ready.

Sample preparation:

Sample was mixed 4:1 with the sample buffer and heated by boiling for 5-10 minutes.

Running the gel:

The gel was clamped in and both the buffer chambers were filled with the running (electrophoresis) buffer. Sample was added into the gel adjusting the volume according to the amount of protein in the sample. Because Coomassie blue was used to stain, very little protein was used to get a nicely defined band.

A lane with molecular weight standards (protein makers) was also included and in this experiment, the standards used were the SM1811 PageRuler Protein ladders (10-250kDa). The power leads were attached and the gel was run until the blue dye front reached ~ 1cm from the bottom of the gel. The PowerPac Universal with 500V/2, 5 A/500W) was used.

The gel was run at 25mA, which needed about one and half hours total runtime. After that, the gel was removed from the power supply and processed further. Proteins were stained using Coomassie brilliant blue solution overnight and then destained using the destaining solution. The gel was kept in distilled water for long periods.

The figures below illustrate the setup used for running of the gels, taken from [PC3267].

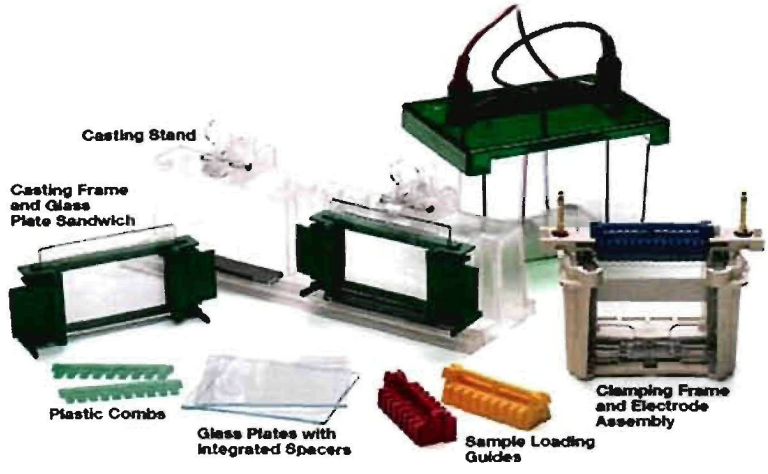

Figure 4.3: Gel Electrophoresis Apparatus

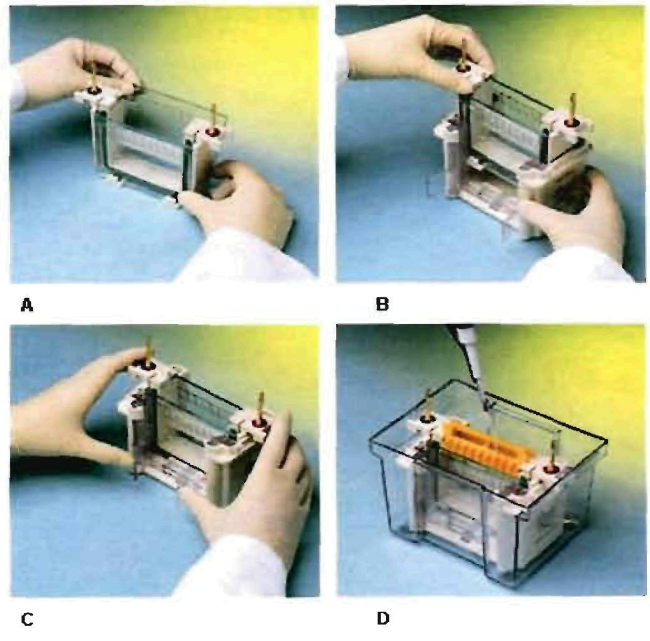

Figure 4.4: Setup of gel in running chamber

4.4.4 Thin-layer chromatography

This technique was performed to illustrate the pigments present in the sample mixture and the following method, taken from Rich et al. [2008] with a few modifications, describes how the experiment was carried out.

Materials needed:

- 1-15ml centrifuge tube with a screw cap
- Erlenmyer flask
- Distilled water
- Hexane
- Small beaker for waste
- Anhydrous Na_2SO_4
- Sample vial
- Pencil
- Ruler
- Cotton or glass wool
- Silica gel TLC plates-microscope slide sized
- Filter paper
- TLC chamber

Method:

1. 10ml of sample and 10 ml of solvent (acetone) were added in a centrifuge tube.

2. The mixture was then centrifuged for 5 minutes at 10 000 g to get the membranes and proteins out, and then transferred to the Erlenmyer flask.

3. 10 ml of hexane was added: the extract was shaken well and left to separate out (one phase was a cloudy, light green lower water layer, while the other phase was a clear, bright green top hexane layer.

4. The water layer was removed and the hexane layer was left in the flask.

5. Another 2 ml of distilled water was added to the hexane layer as a wash.

6. Some anhydrous Na_2SO_4 was added in Erlenmyer flask to dry.

7. The drying agent was removed by filtering it using a Pasteur pipette fitted with a cotton plug.

8. A TLC plate was obtained and a line of about 1cm from the bottom was lightly drawn using a pencil.

9. Capillary tubes were used to make dark enough spots of the extract on the pencil line of the plate.

10. The spotted plate was carefully placed in the TLC chamber that contained a hexane: acetone (7:3, v/v) mixture that was about 0.5 cm deep in the chamber, and the lid was placed on.

Immediately the solvent started moving up the plate. The line of the solvent moving up is called the solvent front. Once the solvent front was within 1cm of the top of the plate, the plate was removed from the chamber, and quickly a mark of the solvent line was made using a pencil.

Most spots on the plate were easily visible by the naked eye, and circled with a pencil. The R_f values of all the spots were determined by measuring the distance from the starting line of the solvent front to the end, then again by measuring to the centre of each spot. The centre spot distance was then divided by the solvent front distance. The higher the R_f value, the less polar the compound.

Figure 4.5: The TLC silica gel plate submerged in a mixture of solvents within a TLC chamber

4.5 Pump-probe setup

Figure 3.1 in Chapter 3 as well Figure 4.7 below; illustrate a generic setup for the pump-probe experiment used in this study. A commercial Ti:Sapphire femtosecond oscillator (Coherent Mira 900-F), operating at a repetition rate of 76 MHz and pumped by the 5 W output of a CW diode-pumped Nd:YVO_4 laser (Coherent Verdi V5), produced pulses of approximately 120 fs duration, as measured by a home-built autocorrelator (see figure below):

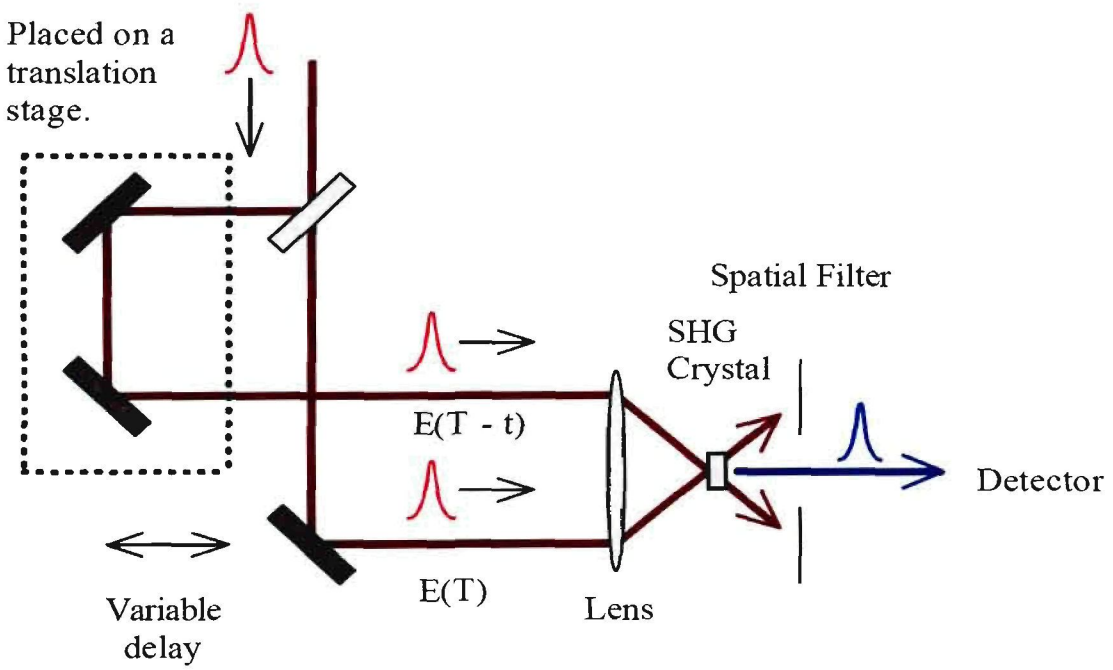

Figure 4.6: A schematic illustration of background free auto-correlation

This is an indirect technique where the pulse is referenced against itself. In this situation, a pulse is replicated and given a time delay with respect to the initial pulse and then sampled against each other. The pulse duration is obtained from the resulting integrated signal. Figure 4.6 above illustrates the setup of a background free auto-correlator where the background signal is removed and only the integrated signal is collected, because the optical path is non-collinear.

These pulses were stretched and then amplified by a regenerative Ti:Sapphire amplifier (Coherent Legend-F) pumped by a diode-pumped, Q-switched Nd:YLF laser (Coherent Evolution) at 1 kHz repetition rate, and finally compressed to produce 120 fs pulses of up to 1 mJ per pulse. This pulse duration was also measured by a home-built autocorrelator shown in Figure 4.6. These pulses have a bandwidth of 11 nm FWHM (full wave half maximum) and a central wavelength of 795 nm.

The amplified beam is split by a beam splitter into two beams (90% transmitted and 10% reflected). These are the pump and probe beams respectively. The probe beam is sent to a variable optical delay line, which comprises a retro-reflector mirror on a precision translation stage controlled by a computer. The probe beam is then focused on a sapphire plate of 2.15 mm thickness to generate a white light supercontinuum.

A short pass filter is placed after this in the probe path in order to suppress the strong residual peak at 795 nm from the Ti:Sapphire laser. The probe beam is split into two beams; the reference and the signal beams. The signal is focused on the sample in such a way that it overlaps spatially with the pump beam in the liquid sample, while the reference beam is also sent through the sample as indicated in Figure 3.1 in Chapter 3.

The pump pulse is sent through an optical parametric amplifier (TOPAS C - OPA) in order to obtain a wide tuning range of the pump beam (530-20000 nm). After the OPA, a chopper is inserted in the pump beam path in order to record spectra that are classified as pumped and not-pumped, thereby reducing background effects.

The probe reference and signal beams are focused on optical fibres that guide the beams into the entrance slit of an imaging spectrometer. The spectrometer (MS 2004 I) uses a Czerny-Tuner optical configuration. The light, after passing through entrance slit, is directed by a collimating spherical mirror onto a diffraction grating. The spectrometer has two gratings for use at different spectral resolutions.

These are a 600 lines/mm diffraction grating blazed at 500nm for 330nm-1000nm operation (multi-channel detection) and a grating 300 lines/mm grating blazed at 1000nm for 700nm-1900nm operation (single-channel detection). The grating disperses the incidence parallel beams (signal and reference beams), and these are again collimated using a second collimating mirror, onto two vertically separated photodiode arrays.

This spectrometer disperses both beams to a maximum of 206 nm. The photodiodes have a pixels height of 2.5 mm and are arrayed at a spacing of 25μm. Each array has 1024 pixels and a spectral response range from 200 nm to 1000 nm. In addition these photodiode arrays have a high UV sensitivity (about 2 x 10^4 photon/ pixel x count) with good stability, a low dark current and high saturation charge that allows a reasonably long integration time for the signal. A longer integration time increases the signal and decreases noise by averaging. Figure 4.7 below illustrates the optical layout of the pump-probe set up described above.

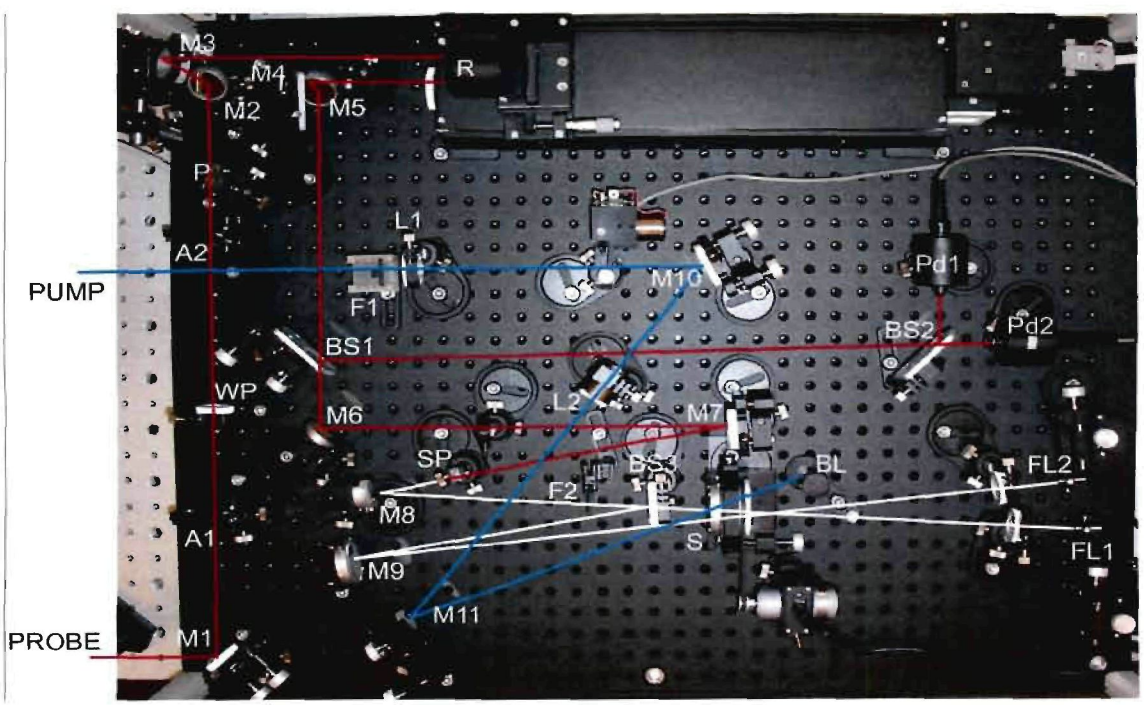

Figure 4.7: Optical layout of the pump probe set up at the NLC

In Figure 4.7 above (adapted from the ExciPro pump-probe user's manual):

M: Mirror
A: Apertures
WP: Half wavelength plate
P: Polarizer
R: Retro-reflector
BS: Beam splitter
SP: Sapphire plate
S: Sample cell
FL: Fibre lead
SH: Synchronised shutter
L: Lenses
BL: Beam locker
B: Berek's variable wave plate
F: Filters

Amplified fundamental pulses enter the ExciPro near mirror M1 and go to M2 through apertures A1 and A2, half wavelength plate WP and polarizer P. A1 and A2 are for easy alignment and they can be removed from the beam using flipper holders. The beam polarizsation is changed (rotated) when WP is rotated. Correspondingly, the pulse energy of selected P horizontal polarisation is changed and adjusted for better continuum generation conditions. Mirrors M2 and M3 form a periscope configuration and direct the beam to the retro-reflector R of the optical delay line.

The second periscope (mirrors M4 and M5) is placed after R and reflects the fundamental beam to the BS1 beam splitter, which reflects a small part of energy to photodiodes PD1 and PD2 placed after another beam splitter BS2. PD1 measures fundamental pulse energy and stability, and PD2 is used for the synchronisation of ExciPro-D electronics.

The main part of the beam is reflected by M6 placed after BS1 and hits concave mirror M7, which focuses the beam into a sapphire plate SP where a femtosecond continuum is generated. The continuum (shown in white) is collimated with the M8 concave mirror and directed to the sample cell S and fibre lead FL1 forming the probe beam. Fifty percent of continuum is reflected from beam splitter BS3 and directed with M9 to S and FL2 forming the reference beam.

Shown in blue the excitation (pump) beam is delivered to the ExciPro from an external wavelength converter like second harmonic generator or optical parametric amplifier. The pump beam goes through the synchronised shutter SH or a chopper installed outside the main unit, and directed to the sample cell with mirrors M10 and M11. The pump beam goes through an iris aperture placed outside the optical unit for better and easy alignment. Lenses L1 and L2 form a telescope for adjusting the pump beam diameter.

The pump beam diameter should always be larger than the probe beam diameter. The pump and probe beam coinciding is achieved with M11. The residual (after the sample cell) pump beam is absorbed with beam locker BL. The Berek's variable wave plate B can be placed between M10 and S to change excitation polarisation for transient absorption anisotropy measurements. Neutral density and colour filters F1 and F2 can be placed into the probe and pump channels.

One can see from Figure 2 that the optical path of the probe beam inside the ExciPro-T optical unit is much larger than the path of the excitation beam. It means that additional optical delay should be achieved for the pump beam outside the unit.

CHAPTER 5

Experimental results and discussion

Introduction

From the various characterisation techniques employed to investigate what the prepared sample contained and if it can undergo long-range energy transfer or any kind of energy transfer processes (suitable for pump-probe experiments), the following results have been obtained and discussed.

5.1 Absorption spectrum

The absorption spectrum of extracted LHC II from spinach leaves measured at room temperature with a UV-1650 PC UV-VIS spectrophotometer is shown below in Figure 5.1. The spectrum indicates that LHCII has a strong absorption on the blue (400-500nm) and the orange-red (600-700nm) part of the spectrum.

Chlorophyll a absorbs strongly around 400-450nm and around 600-700nm, while chlorophyll b absorbs around 430-500nm and 630-680nm. Therefore, the peak at 675 nm is mainly because of chlorophyll a and a shoulder at around 650nm is due to chlorophyll b, the main peak at ~ 440nm is mainly because of chlorophyll a and a shoulder at around 470nm is due to chlorophyll b.

Virtually nothing is being absorbed from the green-yellow-orange wavelengths (500-600nm) by the chlorophylls, but accessory pigments like carotenoids absorbs from 400-500nm. The spectrum is in agreement with what is known in literature [Barzda et al., 1995].

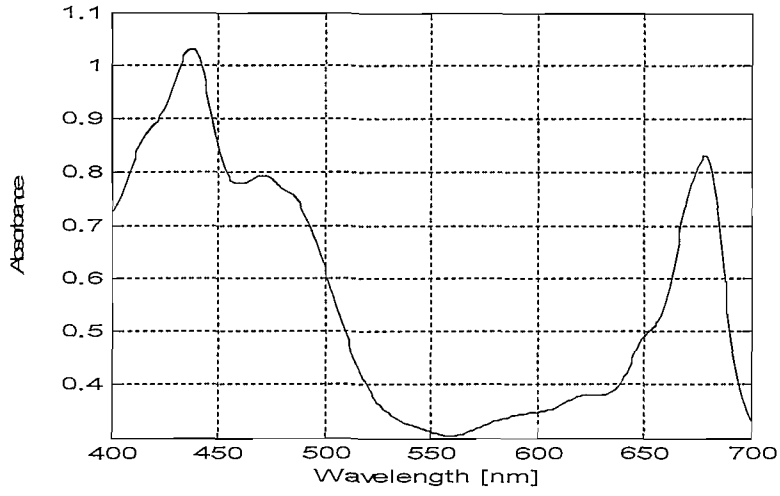

Figure 5.1: Absorption spectrum of extracted LHC II from spinach leaves recorded at room temperature [Barzda et al., 1995]

5.2 Circular dichroism spectroscopy

5.2.1 Absorption spectrum using the Chirascan CD spectrometer

The absorption spectrum of LHC II was also measured simultaneously while the circular dichroism spectrum was measured using the Chirascan spectrometer at room temperature. This was performed mainly to compare the LHC II absorption spectrum taken using a UV-VIS spectrophotometer, and to verify whether the extracted LHC II showed the same absorption spectrum when using a different instrument while measuring the CD spectrum at the same time.

Figure 5.2 below shows the absorption spectrum of extracted LHC II measured using the Chirascan spectrometer at room temperature, and it is similar to the one shown above in Figure 5.1.

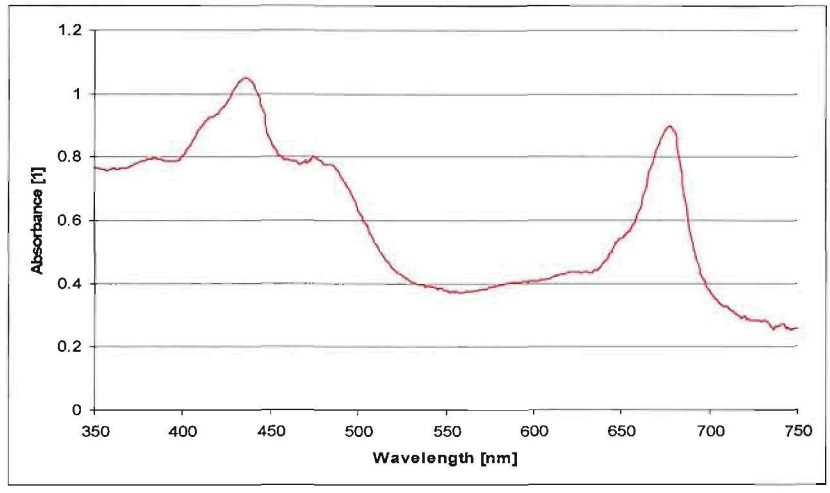

Figure 5.2: Absorption spectrum of extracted LHC II measured using the chirascan at room temperature

5.2.2 Circular dichroism (CD) spectrum

Figure 5.3 below shows the circular dichroism spectrum of extracted LHCII measured at room temperature using the Chirascan CD spectrometer. The chlorophyll content of the sample before dilution was:

- Total Chlorophyll in LHC II = 2.38mg/cm^3
- Chlorophyll a = 1.68 mg/cm^3
- Chlorophyll b = 0.69 mg/cm^3
- Chlorophyll a/b ratio = 2.4: 1

The sample was then diluted with buffer C to give ~1.1 units of absorbance at 440nm and 0.9 at 675nm.

The CD spectrum displays asymmetric bands at wavelengths of interest (675nm and around 430- 505 nm). These anomalous CD bands with psi-type features (smaller amplitudes than in tightly stacked lamellar aggregates), are expected for the loosely stacked lamellar aggregates (type II) [Simidjiev et al., 1997]. This is an essential characteristic of LHC II indicating that there is some degree of organised macro-aggregation of the complexes within the prepared sample to allow energy transfer [(Simidjiev et al., 1997), (Garab et al., 1991)].

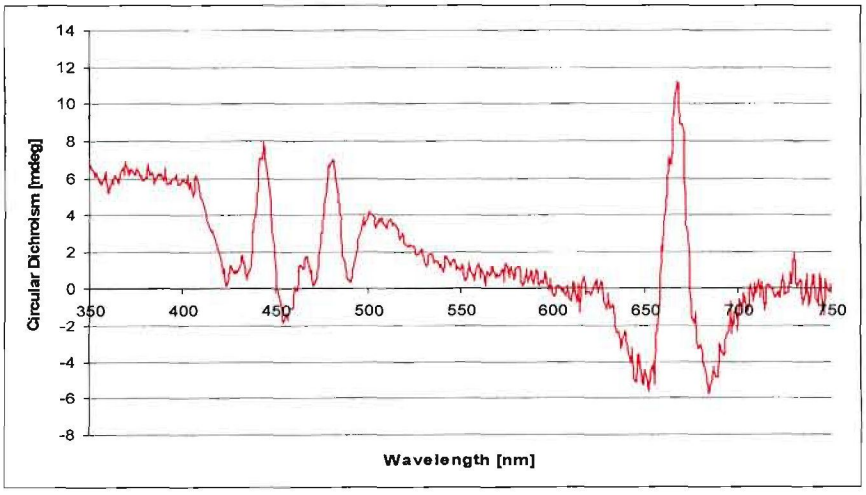

Figure 5.3: CD spectrum of extracted LHC II using chirascan at room temperature

CD spectrum was measured each time a sample was prepared and sometimes at different stages within the preparation method. Figure 5.4 below indicates that lamellar aggregates that were unorganised, disordered and had no intense psi-type CD bands were obtained in some cases, but these samples seemed to have also undergone energy transfer processes.

The CD spectrum taken at the step after adding the detergent during the preparation seemed to give the kind of spectrum showed below. Literature [Simidjiev et al, 1997] showed that adding a detergent of 0.8 – 1% gives disorganised structures of LHC II with aggregates that are tightly packed in big clusters with random distribution. If slightly more detergent was added (not more than 0.9%), it resulted in Figure 5.4 showed below.

This shows that macro-aggregation of LHC II is a necessary, but not sufficient, condition for the long-range order; also macro-aggregation does not disturb the characteristic excitonic CD bands of the LHC II trimers present within the prepared sample [Simidjiev et al, 1997].

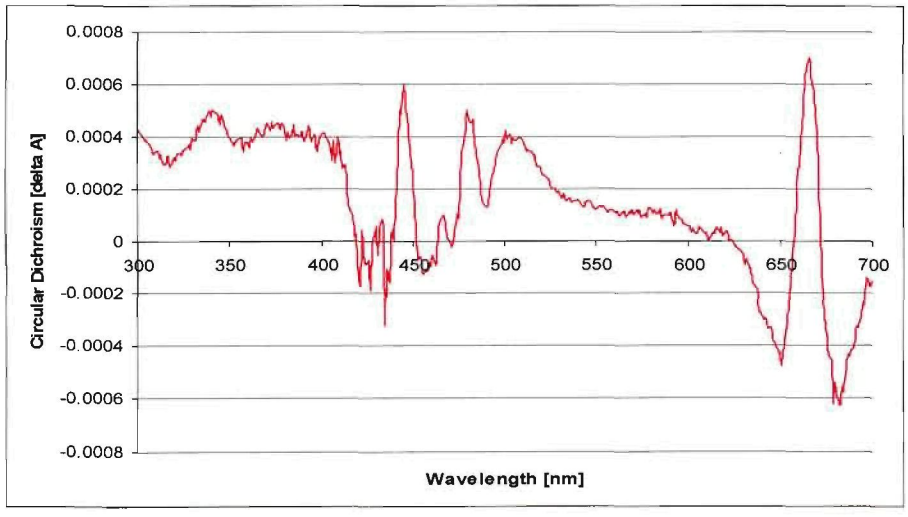

Figure 5.4: CD spectrum of unstacked, disordered lamellar aggregates of extracted LHC II

In terms of the structure of grana (which is a stack of thylakoid membranes where the pigments are situated and photosynthesis occurs), the spectrum in Figure 5.3 indicates that the thylakoid membrane has certain asymmetries (chirality) as in natural systems [Barzda et al., 1994] (see figure below). This structural configuration is important for energy transfer processes.

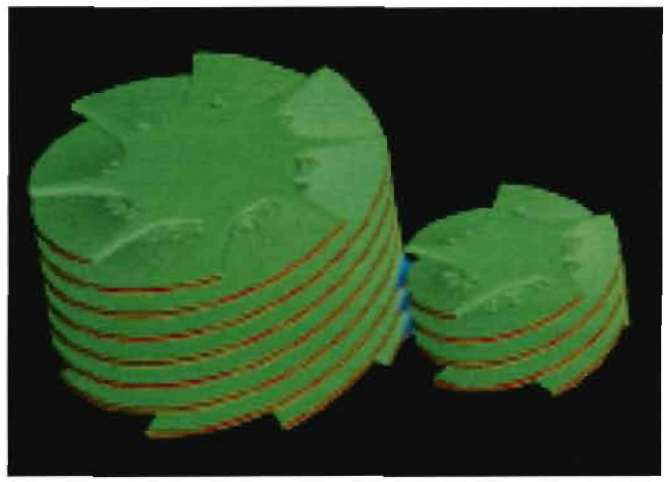

Figure 5.5: The computerised model of grana [(Longman, 1999), (Mustardy & Garab, 2003)]

5.3 SDS-Poly acrylamide gel electrophoresis (PAGE)

Three gel electrophoresis methods were mentioned and discussed in Chapter 3 above. Only the SDS-PAGE (which is the most commonly used method) was performed in this study.

Figure 5.6 below illustrates the results obtained from performing the SDS-PAGE using the extracted LHC II sample at room temperature. Lane 1 contained protein molecular makers, while lanes 2 to 9 contained LHC II sample buffered with a 5x sample buffer in different concentrations to obtain optimal resolution. Lane 2 contained sample that was very diluted (with little protein) and hence very difficult to see using Commassie blue staining solution, while lanes 7 to 9 contained a sample that was more concentrated and thus gave a better resolution.

Note that the gel indicates the presence of small sub-units (20-25 kDa) from LHC I and CPI, as well as the presence of D1 and D2 proteins (which are proteins closely associated with the reaction centre of photosystem II) [Simpson and von Wettstein, 1989]. This implies that the sample did not only contain LHCII, but was contaminated with some components from LHC I as well as some components from the PS II reaction centre.

The prepared sample mostly contained LHC II and this can be seen from the broken down complexes of PS II (see Figure 5.6). CP47 (45k-50kDa) and CP43 (35kDa), which are complexes from the peripheral core complex of PS II, together with D1 and D2 proteins closely associated with the RC were present; pure LHC II (56 kDa) was also present [Simpson and von Wettstein, 1989]. All these pigment protein complexes could be detected using Commassie blue staining solution. Figure 5.6 was taken with a modern digital camera and although the gel was torn (as it was thin and not easy to handle), some results could still be obtained from it.

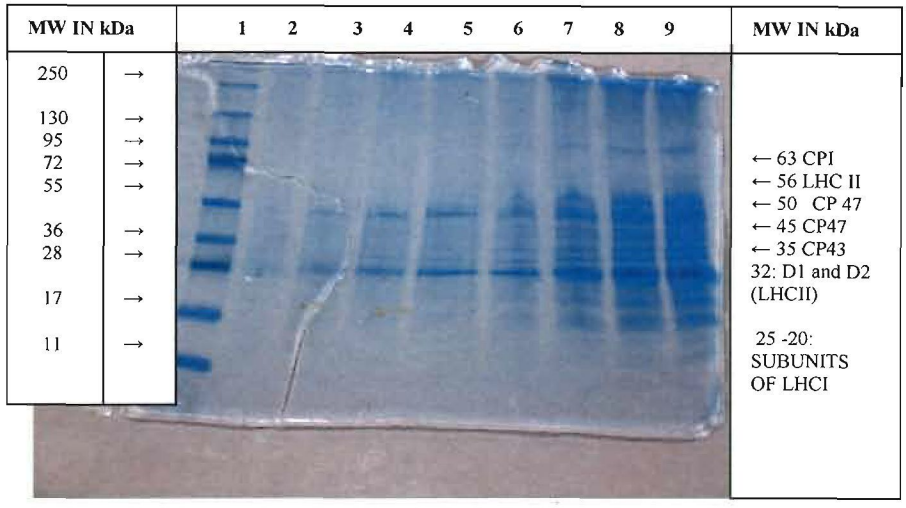

Figure 5.6: SDS-PAGE of extracted sample taken with a modern digital camera

Figure 5.7 below is similar to the SDS-PAGE gel above (Figure 5.6) but scanned using a Vacutec G:Box gel scanner from Syngene, and results analysed using GeneTools software also from Syngene. Lane 1 contained protein molecular makers and lanes 2 to 7 contained LHC II sample in different concentrations for better resolution. Lane 2 contained sample that was more concentrated while lane 6 had very diluted sample (with little protein) and hence was very difficult to see using Commassie blue staining solution. The pigment-protein complexes observed here were similar to the ones discussed above.

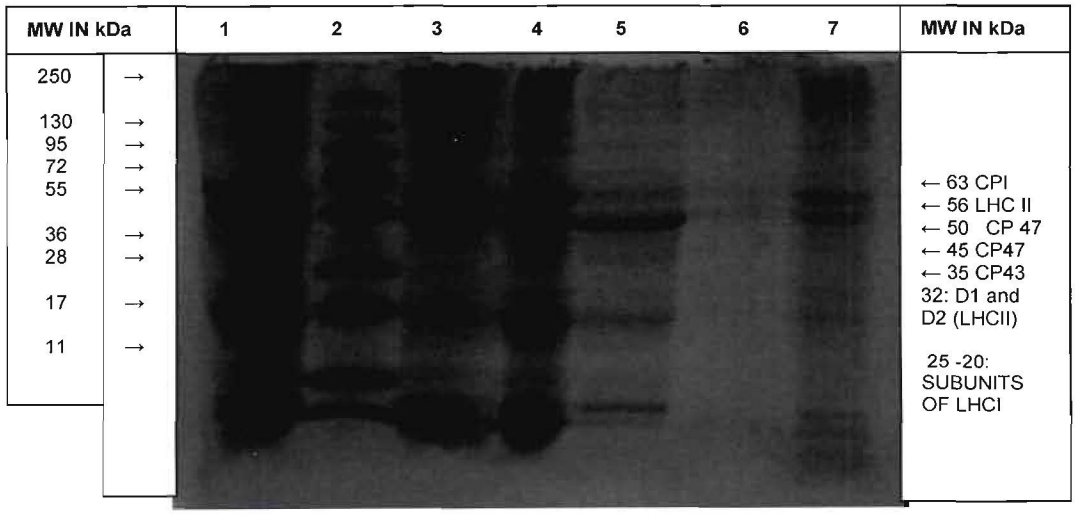

Figure 5.7: SDS-PAGE of extracted sample scanned using a Vacutec G:Box from Syngene

5.4 Thin-layer chromatography (TLC)

Pigment extraction was performed and the analysis was carried out using thin layer chromatography to observe the pigments present in the extracted LHC II sample. In this experiment, a mixture of solvents (hexane and acetone) was used to facilitate the movement of the pigments up the plate (made of silica gel beads). This is because these solvents are non-polar, and most photosynthetic pigments are also non-polar hence "like dissolves like" [Rich et al,]. The pigment that had the highest affinity for the TLC plate moved the furthest on the plate (migration is from bottom to top of the TLC plate).

Figure 5.8 below illustrates the pigments contained in the prepared LHC II sample. Chlorophyll a, which is the primary pigment of all photosynthetic systems, was present in the mixture, as well as other accessory pigments like chlorophyll b, carotenes and xanthophylls. All these accessory pigments assist in the collection of light energy that is not absorbed by chlorophyll a, as there are many pigments for a single reaction centre.

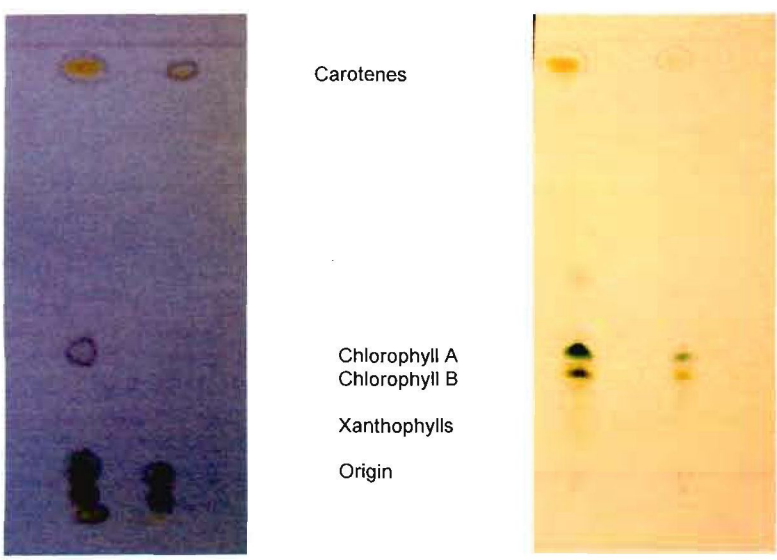

Figure 5.8: Pigments present in LHC II preparation

5.5 Pump-probe spectroscopy

After the characterisation methods (UV-VIS absorption spectrum, CD, SDS-PAGE and TLC) revealed that LHCII was contained in the prepared sample, the sample was ready for the pump-probe experiments (as described in Chapter 4). Figure 5.9 below shows the transient absorption spectra for the LHC II extracted from spinach leaves measured at room temperature for the red part of the spectrum. Both the graphs were drawn from the same set of data.

The absorption change (Δabs) vs. wavelength (λ) graph is presented in Figure 5.9a, where the different colours in the graph represent different probe delay times. The maximum absorption of LHC II on the red part of the spectrum is at 680nm (see Figure 5.1). The graph shows a negative band at this wavelength, which is due to ground state bleaching (GSB) of chlorophyll molecules [Vengris, 2005].

Figure 5.9b represents the Δabs vs. time graph. Data points at zero represent the processes before the pump is introduced, and as soon as the pump is introduced, at 610nm in this particular case, the ΔAbs drops until it reaches a minimum. In theory, at this point all the molecules are in the excited state, and there is little or no molecules left in the ground state to absorb the energy.

After this, the ΔAbs returns to its original (zero) state after some time, as most molecules have now dropped back to the ground state. The energy that they possessed has now been passed on to the next available energy acceptor or released as fluorescence if there were no energy acceptors available.

Two exponential fits were obtained using this set of data and gave two time constants t_1 and t_2.

$$t_1 = 2.27 \pm 1.32 \text{ ps}$$
$$t_2 = 14.46 \pm 5.31 \text{ ps}$$

The 2.27 ps time constant can be ascribed to singlet-singlet annihilation within LHC II monomer, while the 14.46 ps component can be ascribed to the annihilation in the trimer. These time values of annihilation have been observed at 679 nm in literature [(Barzda et al., 2001), (Croce et al., 2001)].

Comparing our results with what is known in literature shows that our results correlate well. The time constant of 2-3 ps and ~ 17 ps for the excitation transfer processes at 678 nm in higher plants has been observed [de Weert et al., 2002]. Time constants of ~ 2.27 ps and ~ 14.46 ps at 680 nm were observed in this study.

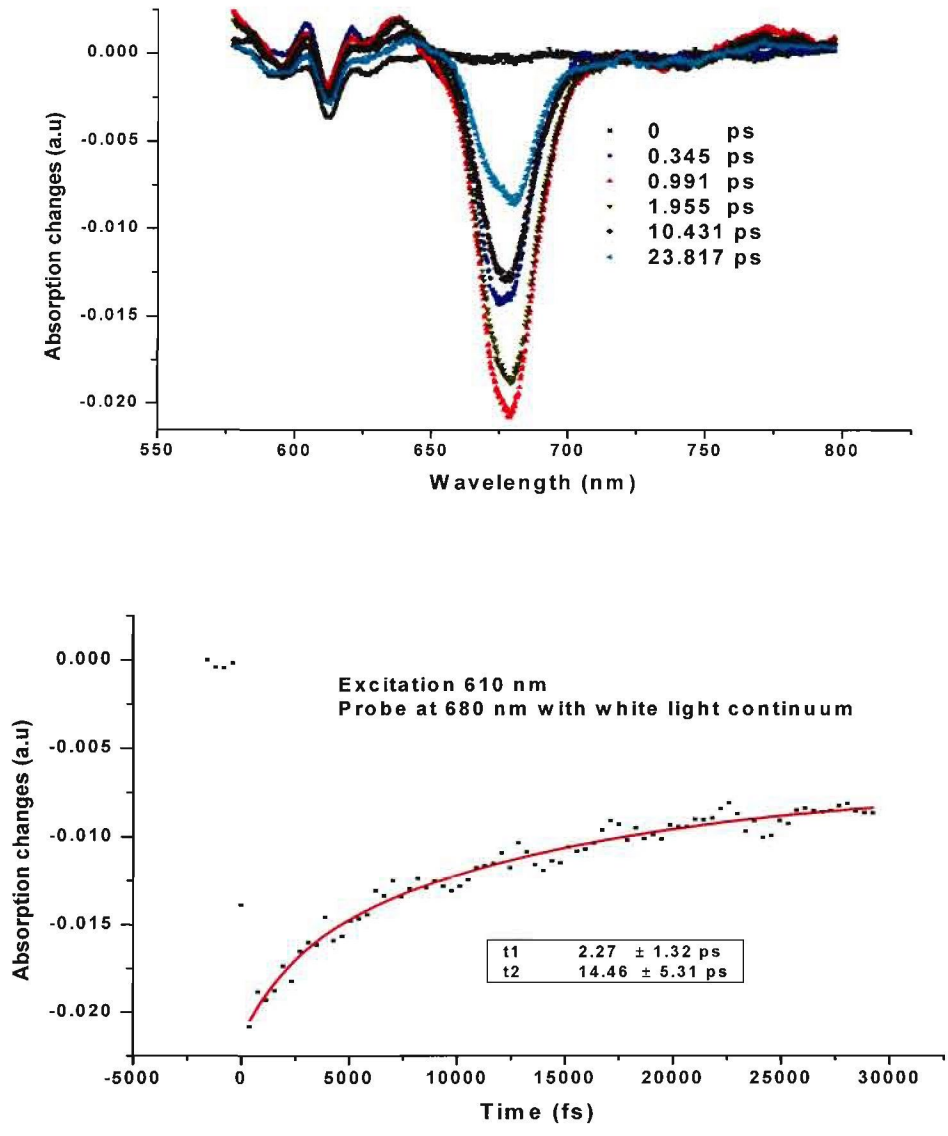

Figure 5.9: a) Absorption change (Δabs) vs. wavelength (λ) and b) Δabs vs. time graph

More work was carried out using the extracted LHC II over the entire spectral range of LHC II (400-700nm).

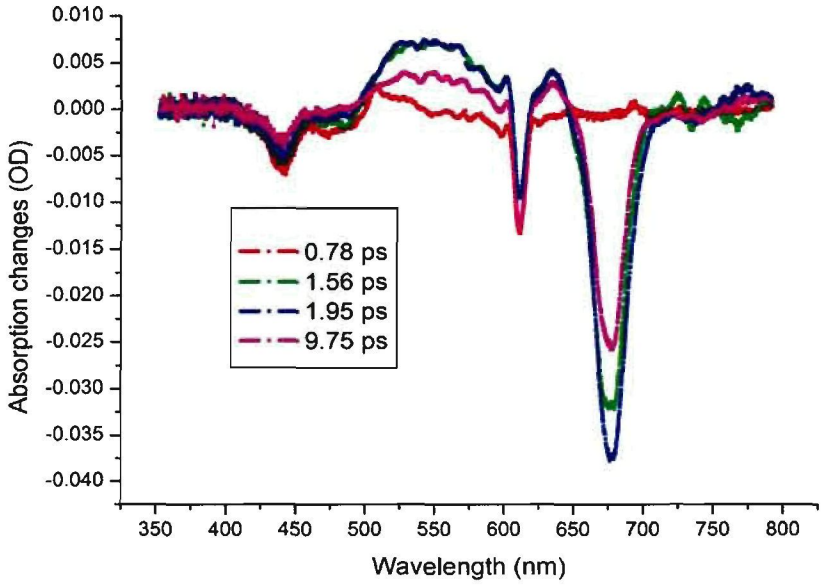

Figure 5.10: Transient absorption spectra of extracted LHCII in the wavelength region 350-800nm and different time delays

Figure 5.10 above illustrates the transient absorption spectra of extracted LHC II from spinach leaves, measured at room temperature. In this particular experiment, the pump beam was set at 610 nm and the probe was a white light continuum. From the data presented in Figure 5.10, a positive band at ~542 nm and three negative bands at ~ 436 nm, 610 nm and 678 nm can be observed.

A negative shoulder is also observed around 472nm. The negative changes at 436 nm and 678 nm could be due to the ground state bleaching (GSB) as was explained when Figure 5.9 was discussed. The positive band at 542nm on the other hand is representative of the excited state absorption (ESA) of the chlorophyll molecules within the LHCII [Vengris, 2005].

The negative band observed at 610 nm could be due to the scattered laser light caused by some small solid particles observed in the liquid sample. These small particles in the samples were observed if the prepared sample had been stored for long periods of time (more than a month) after the preparation date, even if it was stored in recommended conditions, such as extremely cold temperatures and in the dark. Except for the huge scattering of laser light at 610nm, these old samples also gave the same pattern of results as the freshly prepared sample. The shoulder observed at ~ 472 nm can be accounted for by stimulated emission (SE) [Vengris, 2005].

Information about the time constants for the situation above was also extracted from the data. Second order exponential fit procedure to the data sets obtained at 436 nm, 472 nm, 542 nm and 675 nm, was applied (see figure 5.11 below) as single exponential fit did not fit the data well.

The results of the second-order exponential fit revealed two time constants for each wavelength;

436nm: 0.39 ps and 5.26 ps
472 nm: 0.64 ps and 6.38 ps.
542 nm: 0.45 ps and 8.05 ps.
678 nm: 1.33 ps and 24.55 ps.

In each case, the faster time constant can be ascribed to singlet-singlet annihilation within LHC II monomer, while the slower component can be ascribed to the annihilation in the trimer [(Barzda et al., 2001), (Croce et al., 2001)].

To get these time constants and the data used to extract them, the spectra are often measured at a large number of delay times so that the fast absorption changes can be temporally quantified (extraction of the time constants). Figure 5.11 below illustrates the evolution of the absorbance changes at 678 nm (maximum absorption in Figure 5.10), 542 nm, 472 nm as well as 436 nm, as a function of time.

In the 678 nm, 472 nm and 436 nm bands, there is a fast decrease (drop) in the absorbance change until a minimum is reached, which is then followed by a slow recovery. In the 542nm band, a fast increase is observed, which is subsequently followed by a slow downturn. The time constant was then extracted from these graphs using the second order exponential fit procedure.

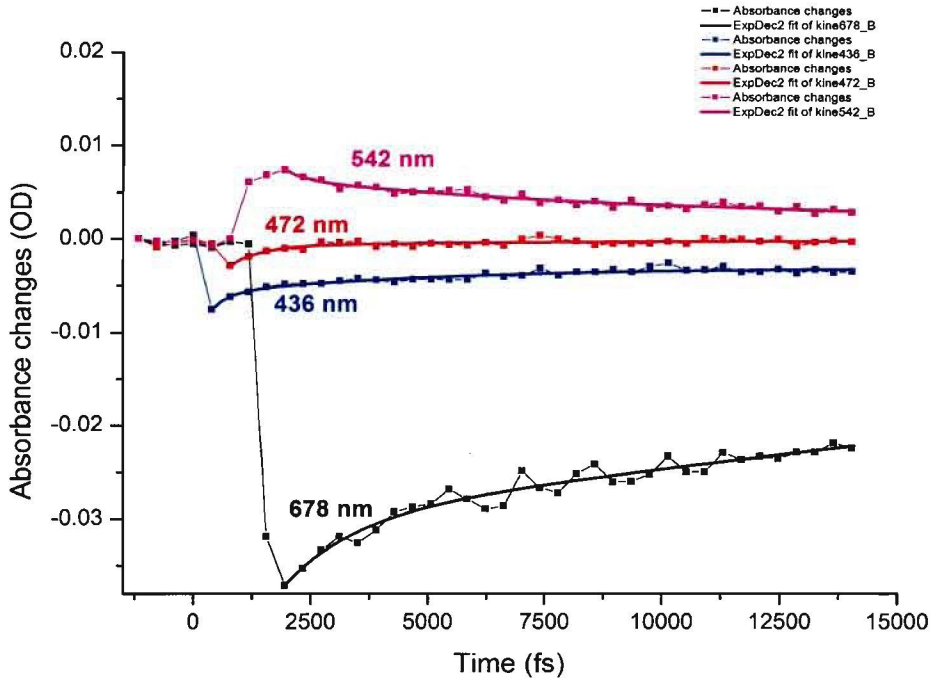

Figure 5.11: Absorbance at 436 nm, 472 nm, 542 nm and 678 nm as a function of delay between the pump and probe pulses in LHC II

Figure 5.12 below shows similar results as Figure 5.11, the difference being that in Figure 5.12, there is no chirp. Chirp, in simple terms, is a physical effect whereby a laser pulse is broadened upon contact with a medium (in this particular case, a sapphire plate) and hence the pulse duration is increased. Taking measurements without chirp in the laser pulse helps in a sense that all the peaks on the red and blue part of the spectrum appear at the same time.

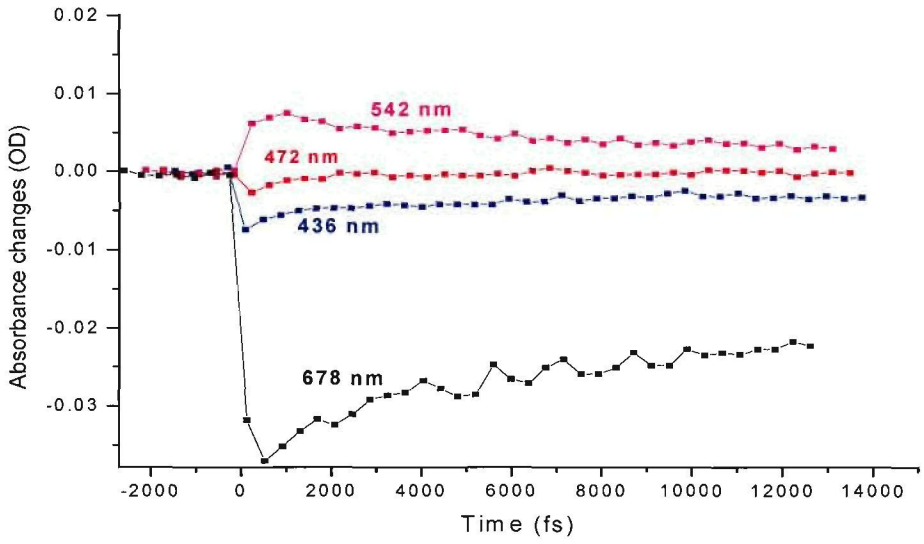

Figure 5.12: Absorbance at 436 nm, 472 nm, 542 nm and 678 nm as a function of delay between the pump and probe pulses in LHC II without chirp

The transient absorption was also carried out at different pump wavelengths. Figure 5.13 below illustrates the absorbance changes of the same sample that contained extracted LHC II pumped at different wavelengths (610 nm, 630 nm, 650 nm and 680 nm at zero delay time or strongest absorption time). The strongest absorption change of about 0.052 OD was observed when the pump was set at 680 nm. When the pump was set at 630 nm and 650 nm, this produced absorption changes of 0.027 OD and 0.020 OD, respectively.

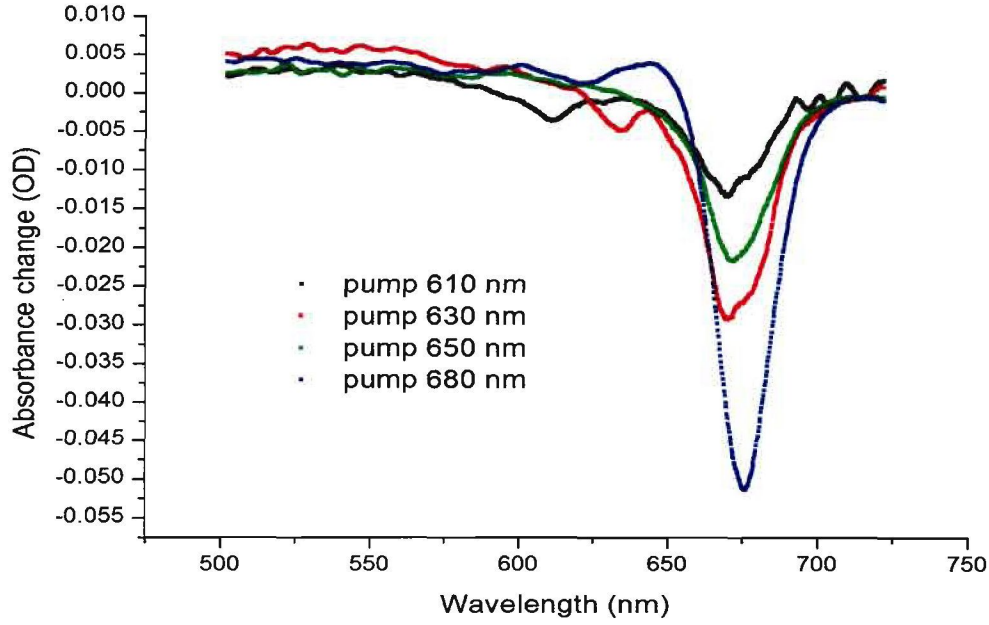

Figure 5.13: Transient absorption of extracted LHC II for different pump wavelengths

A combination of the time and wavelength dependant spectra produces a three-dimensional contour plot presented in Figure 5.14 below. This graph contains information for all measured wavelengths. It shows a scattered laser signal at 610 nm, which is not time dependent, and is probably due to the scattered laser light caused by small solid particles observed in the liquid sample. In addition, it indicates negative absorbance changes at 678nm and 436 nm that could be the result of the ground state bleaching (GSB) of chlorophyll molecules. Some positive absorbance changes that were observed at 542 nm could be due to the excited state absorption (ESA) as explained before. Finally, the negative shoulder observed at ~ 472 nm may be accounted for by stimulated emission (ES) [Vengris, 2005].

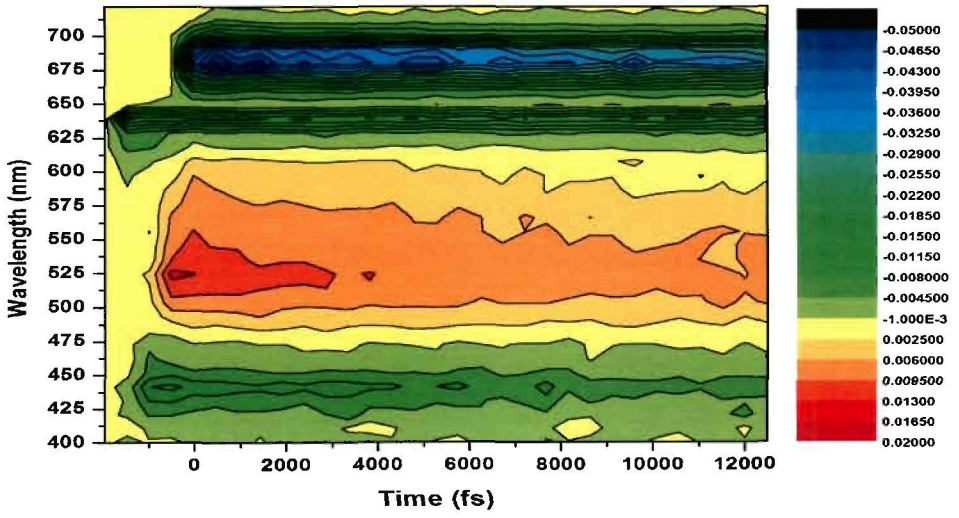

Figure 5.14: Transient absorption contour graph indicating measured absorbance spectra for a range of delay times between pump and probe pulses

CHAPTER 6

Conclusions and future work

6.1 Conclusions

Based on the results obtained and discussed during this study, the following conclusions can be drawn:

- Light harvesting complex II that could undergo energy transfer processes, was successfully extracted from spinach leaves using Krupa's method. This was supported by evidence obtained from the UV-VIS absorption spectrum, CD spectrum, SDS-PAGE, TLC and the pump-probe (transient absorption spectra) experiments used to characterise the prepared sample (see Chapter 5).

- The pump-probe results (Chapter 5.5) obtained from this study assisted in benchmarking and calibrating the pump-probe system developed at the National Laser Centre (CSIR) in 2007. The results obtained when using the extracted LHC II sample corresponded to what is known in literature [(van Grondelle and Amesz, 1986), (Barzda et al., 2001)], hence it provided a good starting point to continue using the artificial photosynthetic systems still to be developed at Biosciences (CSIR).

- The absorption spectrum of the extracted LHC II sample was measured using two instruments (the UV-VIS spectrophotometer and Chirascan spectrometre), and the results indicated strong absorption bands at around 400 nm - 500 nm and again at around 600 nm - 700 nm. This spectrum is in agreement with what is typical of a LHC II sample and documented in literature [(Auderisk and Byers, 2005), (Barzda et al., 1995)].

- After confirming that the sample contained LHC II in it by means of measuring the absorption spectra (see Figure 5.1), a circular dichroism (CD) spectrum was used to evaluate if the sample had formed aggregates important for the energy transfer processes.

- The CD spectrum (Figure 5.3) showed asymmetric bands at two wavelength regions, one around 430 nm - 505 nm and the strongest one at around 675 nm. These CD bands had psi-type features indicating the presence of large macro-aggregates with long-range chiral order important for long-range energy transfer [(Garab et al., 1991), (Simidjiev et al., 1997)].

- In terms of the structure of the grana (which is a stack of thylakoid membranes where the pigments are situated), the information obtained from the CD spectrum (Figures 5.3 and 3.6) showed that the thylakoid membrane has certain asymmetries (chirality) as in natural systems (Figure 5.5), which is ideal for successful energy transfer processes [(Longman, 1999), Mustardy and Garab, 2003)].

- SDS-PAGE (Chapter 5.3) illustrated the presence of minor complexes from LHC I as well as proteins that are closely associated with the reaction centre (D1 and D2 proteins), indicating that the prepared sample contained not only LHC II, but was also contaminated with a bit of LHC I and the RC [Simpson and von Wettstein, 1989].

- Thin-Layer chromatography (Chapter 5.4) showed the presence of essential pigments during the energy transfer processes of photosynthesis. Chlorophyll a (primary pigment of most photosynthetic systems) was spotted on the TLC plate. Chlorophyll b as well as other accessory pigments such as carotenes and xanthophylls was also present in the extracted LHC II sample. All these pigments participate in the collection of light energy and transfer to the reaction centre [Rich et al., 2008].

- Pump-probe experiments illustrated that the extracted LHC II sample indeed underwent energy transfer processes (Chapter 5.5). The sample contained two separate energy transfer mechanisms with different time constants; the faster time constant that could be ascribed to singlet-singlet annihilation within LHC II monomer, and the slower component that could be ascribed to the annihilation in the trimer.

- When focusing only on the red part of the spectrum, (performed as preliminary experiments), the absorption change vs. wavelength graph (Figure 5.9a) showed a negative band at 680 nm, which could be because of the ground state bleaching (GSB) of chlorophyll molecules [Vengris, 2005]. Absorption vs. time graph (figure 5.9b) indicated two time constants; $t_1 = 2.27 \pm 1.32$ ps, which corresponded to the singlet-singlet annihilation within LHC II monomer and $t_2 = 14.46 \pm 5.31$ ps, which corresponded to the annihilation in the LHCII timer. Both these time constant are in agreement with what is known in literature [Barzda et al., 2001].

- Focusing on the whole spectral range where LHC II is active (400 nm- 700 nm), the absorption change vs. wavelength graph (Figure 5.10) showed three negative bands (at ~ 436 nm, 610 nm and 678 nm) and a positive band at ~ 542 nm; there was also a negative shoulder at ~ 472 nm. The negative bands at 436 nm and 678 nm as discussed in Chapter 5.5 could be due to the ground state bleaching (GSB) of chlorophyll molecules, while the 610 nm negative band could be due to the scattered laser light caused by small solid particles observed in the liquid sample (these solid particles started to form when the sample was stored for over a month). A positive band at 542 nm can be viewed as a representative of the excited state absorption (ESA) of chlorophyll molecules within LHC II. The shoulder observed at 472 nm could be accounted for by stimulated emission (Figure 3.2).

- Second order exponential fit procedure was applied to the data sets obtained at 436 nm, 472 nm, 542 nm and 675 nm to extract the time constants for the situation above. The following results were obtained:

436nm: 0.39 ps and 5.26 ps

472 nm: 0.64 ps and 6.38 ps.

542 nm: 0.45 ps and 8.05 ps.

678 nm: 1.33 ps and 24.55 ps.

In each case, the faster time constant can be ascribed to singlet-singlet annihilation within LHC II monomer, while the slower component can be ascribed to the annihilation in the trimer [Barzda et al., 2001].

6.2 Recommendations for future work

This project was performed to do preliminary work paving the way for the main objective of the overall project, which is to develop artificial functional light harvesting arrays and energy transfer systems that mimic the photosynthetic process in nature, in order to enable us to use the sun as a clean, neutral and carbon-free source of energy.

Based on the work performed in this study, the results obtained and the conclusions made, the following recommendations for future work can be drawn:

- Other light harvesting complexes (LHC I) as well as photosystems (PS I and II) can be used and their energy transfer pattern studied using the pump probe experiments. LHC II was selected in this particular case, as it is well characterised, hence easy to use in helping to benchmark the pump-probe system installed at the National Laser Centre.

- Characterisation methods are available from a biological point of view (SDS-PAGE, CD, UV-VIS spectroscopy and TLC) to characterise the prepared samples before performing the pump-probe experiments.

- The process of designing and developing artificial light harvesting arrays and energy transfer systems is already in place and this project is a collaboration between the Synthetic Biology Group and the National Laser Centre at the Council for Scientific and Industrial Research (CSIR) Campus.

- Katterle and co-workers [Katterle et al., 2007] published a paper in 2007 entitled *An artificial supramolecular photosynthetic unit*. This unit can be viewed as a conceptual approach to self-assembled supramolecular solar cells, utilising bio-inspired materials as a starting point for advanced solar energy conversion units. This unit also provides the following insight: that there are other groups around the world that are working on artificial arrays and that it is possible to build such a solar cell.

- The future plan of our group is to incorporate *Bacteriodopsin* in developing these systems as well as a polymer backbone. At this stage, not much information can be given as this is still in the planning stage.

List of references:

Allen, K. D., and Staehelin L.A., (1992). *Biochemical Characterization of Photosystem II Atenna Polypeptides in Grana and stroma Membranes of Spinach.* Plant Physiol, 100, 1517-1526.

Amesz, J., and Hoff, A., (eds.), (1996). *Biophysical Techniques in Photosynthesis.* Kluwer Academic, the Netherlands.

Amesz, J., (1987). *Photosynthesis.* Elsevier, Amsterdam.

Amunts, A., Drory O., Nelson N., (2007). The *structure of a plant photosystem I supercomplex at 3.4Å resolution.* Nature, Vol 447, 58-63.

Arnon, D. J., (1949). *Copper enzymes in isolated chloroplasts: polyphenoloxidase in Beta vulgaris.* Plant Physio. 24, 1-15.

Auderisk T. and Byers, (2005). Bellevue Community College, Washington USA, Biology *101 lecture notes*, Chapter 7, page 4-5, from *Biology: Life on Earth*, 7th.

Bailey R. E, PhD, (2006). *Photosynthesis study guide*, Biology Department, Central Michigan University.

Baker, N. (ed.), (1996). *Photosynthesis and the Environment.* Kluwer Academic, Netherlands.

Barber, J., (ed.) (1992). *The Photosystems: Structure, Function and Molecular Biology*, Elsevier, Amsterdam.

Berg, J.M., Tymoczko J.L., Stryer L., (2002). *Biochemistry textbook, fifth (international) Edition.* W.H Freeman and Company.

Berova, N., Nakanishi K., Woody R. W., (2000). *CD Principles and Applications 2nd edition*, A John Wiley & Sons, Inc., Publication, ISBN 0-471-330035.

Barzda V., Gulbinas V., Kananavicius R., Cervinskas V., van Amerongen H., van Gr Rondelle R. and Valkunas L. (2001). *Singlet-singlet Annihilation Kinetics in Aggregates and Trimers of LHCII.* Biophysical Journal, Vol 80: 2409-2421.

Barzda, V., Garab, G., Gulbinas, V., Valkunas, L., (1995). *Evidence for long-range excitation energy migration in macroaggregates of the chlorophyll a/b light harvesting antenna complexes.* Biochimica et Biophysica Acta 1273, 231-236.

Barzda, V., Mustardy, L., Garab, G., (1994). *Size dependency of circular Dichroism in macroaggregates of photosynthetic pigment-protein complexes.* Bio-chemistry 33, 10,837-10,841.

Blankenship, R. E., and Parson, W. W., (1979). *The involvement of iron and ubiquinone in electron transfer reactions mediated by reaction centers from photosynthetic bacteria.* Biochim. Biophys. Acta **545**, 429-444.

Blankenship, R.E. (1996). *Photosynthetic antennas and reaction centers: Current understanding and prospects for improvement.* In Nozik, A.J., Ed. Research Opportunities in Photochemical Sciences.

Bollag, D.M., Rozycki, M.D. and Edelstein, S.J. (2002). *Protein Methods, 2nd ed.* Wiley-Liss, Inc. New York. pp. 149.

Butler, P.J.G., and Kuhlbrandt, W., (1988). Proc. Natl.Acad.Sci.USA.85,3797-3801.

Campbell N, Reece J. (2002). *Biology, 6th ed.* Pearson Education, Inc. San Fransisco, CA.

Carpentier R., (2006). *Photosynthesis Research Protocols*, Département de chimie biologie Université du Québec à Trois-Rivières, Québec, Canada

Coligan, J.E., *et al.*, Eds., (2002). *Electrophoresis, In Current Protocols in Protein Science,* pp. 10.0.1-10.4.36. John Wiley and Sons, Inc. New York.

Croce R., Müller M.G., Bassi R. and Holzwarth A.R. (2001). Carotenoid-to-chlorophyll energy transfer in recombinant major light-harvesting complex (LHCII) of higher plants. I. Femtosecond transient absorption measurements. *Biophysical Journal* **80,** 901-915.

Croce, R., Weiss, S., Bassi, R., **(1999)**. *J. Biol. Chem. 274*, 29613.

Damjanovic A, Ritz T, and Schulten K., (2000). *Excitation energy trapping by the reaction center of* Rhodobacter sphaeroides. Int. J. Quantum Chem., 77:139-151.

Damjanovic, A., Ritz, T., and Schulten K., (1999). *Energy transfer between carotenoids and bacteriochlorophylls in a light-harvesting protein.* Phys. Rev. E **59**:3293–3311.

Debus, R.J., Feher, G., and Okamura, M.Y., (1986). *Iron depleted reaction centers from Rhodopseudomonas sphaeroides R26.1: Characterization and reconstitution with* Fe^{2+}, Mn^{2+}, Co^{2+}, Ni^{2+}, Cu^{2+}, *and* Zn^{2+}. Biochemistry **25**, 2276-2287.

Deisenhofer, J. and Michel, H. (1992). *High resolution crystal structures of bacterial photosynthetic reaction centers.* In Ernster, L., Ed. Molecular Mechanisms in Bioenergetics. Elsevier, Amsterdam, pp. 103-120.

Dekker J.P., Boekema E.J. (2004). *Supramolecular organisation of thylakoid membrane proteins in green plants.* Biochimca et Biophysica Acta 1706 (2005) 12-39.

de Weerd F. L., van Stokkum I. H. M., van Amerongen H., Dekker J.P., van Grondelle R., (2002). *Pathways for Energy Transfer in the Core Light-Harvesting Complexes CP43 and CP47 of Photosystem II.* Biophysical Journal, pages 1586 -1597, Vol 82.

Dexter, D.L. (1953). *A theory of sensitized luminescence in solids.* J. Chem. Phys.**21**:836–850.

Dong-Hui Q., Shi-Lin L., Lei Z., Jian Y., Li W., Guo-Zhen Y. and Yu-Xiang W., (2003). *Experimental study on the chirped structure of the white-light continuum generation by femtosecond laser spectroscopy.* Vol 12, No 9, Chin. Phys. Soc and IOP Publishing Ltd.

Doust.A.B, van Stokkum.I.H.M, Larsen.D.S, Wilk.K.E, Curmi.P.M.G, van Grondelle.R,and Scholes.G.D. 2005. J.Phys.Chem.B vol.109, p14219-14226.

Drews Gerhart , Microbiological reviews, Mar. (1985). *Structure and Functional Organization of Light-Harvesting Complexes and Photochemical Reaction Centers in Membranes of Phototrophic Bacteria,* Vol. 49, No 1, Institute of Biology 2, Microbiology, Albert- Ludwigs University, D-7800 Freiburg, Federal Republic of Germany. p. 59-70.

Duysens, L.N.M., (1952). *Transfer of Excitation Energy in Photosynthesis.* Ph.D. thesis, Utrecht.

Emerson R. and Arnold W., (1932). *The Photochemical Reaction in Photosynthesis.* The Journal of General Physiology Vol 16, 191-205. The Rockefeller University Press.

Engel G. S., Calhoun T. R., Read E. L., Ahn T., Mancal T., Cheng Y., Blankenship R. E., and Fleming R., (2007). *Evidence for wavelike energy transfer through quantum coherence in photosynthetic systems.* Nature Letters, Vol 446.

Farabee, M.J., PhD, (2006): *On-Line Biology Book,* Chapter 13, Date last visited (12/06/07).

Ferreira K.N., Iversion T.M., Maghlaoui K., Barber J., Iwata S. (2004). *Architecture of the photosynthetic oxygen-evolving centre.* Science, 303: 1831-1838

Förster, T. (1948). *Zwischenmolekulare Energiewanderung und Fluoreszenz.* Ann. Phys. (Leipzig) **2**:55 75.

Frank, H.A. (1993). *Carotenoids in photosynthetic bacterial reaction centers: Structure, spectroscopy, and photochemistry.* In Deisenhofer, J. and Norris, J.R., Eds. The Photosynthetic Reaction Center., vol. **II**. Academic Press, San Diego, pp. 221-237.

Garab, G., Kieleczawa, J., Sutherland, J.C., Bustamante, C, and Hind, G. (1991). Photochem. Photobio. 54,273-281.

Garab, G., Faludi-Daniel A., Sutherland J. C., and Hind G., (1987). *Macroorganisation of Chlorophyll a/b Light-Harvesting Complex in Thylakoids and Aggregates: Information from Circular Differential Scattering.* Biochemistry, 27, 2425-2430.

Garrett & Grisham, (1999). *Biochemistry, 2nd Edition,* Chapter 22, Saunders College Publishing, 1127p.

Gradinaru.C.C, Kennis.J.T.M, Papagiannakis.E, van Stokkum.I.H.M, Cogdell.R.J, Fleming.G.R, Niederman.R.A and van Grondelle.R. 2001. PNAS. Vol.98. p2364-2369.

Groot.M.L, Breton.J, van Wilderen.L.J.G.W, Dekker.J.P and van Grondelle.R. 2004. J.Phys.Chem.B vol.108 p8001-8006.

Hall, D.O. and K.K. Rao (1994). *Photosynthesis.* Cambridge University, Press, Boca Raton, FL.

Hames, B.D. and Rickwood, D. Eds. (1990). *Gel Electrophoresis of Proteins: a Practical Approach, 2nd ed.* Oxford University Press, New York.

Hiyama, T., (1996). *Photosystem I: structures and functions, in Handbook of Photosynthesis* (Pessarakli, M.ed), Marcel Dekker, New York, pp. 195-217.

Humphrey, W.F., A. Dalke, and K. Schulten. (1996). VMD — *Visual Molecular Dynamics*. J. Mol. Graphics **14**:33–38.

IUPAC Nomenclature for Chromatography, IUPAC Recommendations (1993). *Pure & Appl. Chem.,* Vol. 65, No. 4, pp.819-872. 1993. Printed in Great Britain.

Iwata S. and Barber J, (2004). *Structure of photosystem II and molecular architecture of the oxygen-evolving centre,* Current Opinion in Structural Biology 2004. 14: 447 – 453.

Katterle M., Prokhonrenko V., Holzwarth A. and Jesorka A., (2007). Chemical Physics Letters 447, 284-288.

Kim, M., Ulibarri, OL., Keller, D., Maestre, M.F., and Bustamante, C. (1986), J. Chem. Phy. 84, 2981-2989.

Kiss, J. G., Garab, G., Toth, Zs., and Faludi-Daniel, A. *(1986).* Photosynth. Res. 10, 217-222.

Krupa, Z., Huner, N. P. A., Williams, J. P., Maissan, E., and James, D. R (1987). *Development at cold hardening temperatures-the structure and composition of purified rye LHCII.* Plant Physiol.84, 19-24.

Kuhlbrandt, D.N., Wang, and Fujiyoshi Y., (1994*). Atomic model of plant harvesting complex by electron crystallography.* Nature 367:614-621.

Lacks, S. A., Springhorn S. S., and. Rosenthal A. L., (1979). *Effect of the composition of sodium dodecyl sulfate preparations on the renaturation of enzymes after polyacrylamide gel electrophoresis.* Anal. Biochem. 100:357-363.

Lee. H, Cheng.Y-C and Fleming G.R. 2007 Science 316 p.1462 – 1465.

Liu Z., Yan H., Wang K., Kuang T., Zhang J., Gul L., An X. and Chang W. (2004). Crystal structure of spinach major light-harvesting complex at 2.72 Å resolution. *Nature* **428**, 287–292.

Longman, A.W, (1999). *Structures of the plant cell.*

Mančal.T, Valkunas.L, Read.E.L, Engel.G.S, Calhoun.T.R and Fleming.G.R. 2008 Spectroscopy 22 p.199 – 211.

Miller, K.R. (1982). *Three-dimensional structure of a photosynthetic membrane.* Nature **300**:53–55.

Monger, T. G., and Parson W. W. (1977). *Singlet-triplet fusion in Rhodopseudomonas sphaeroides chromatophores. A probe of the organization of the photosynthetic apparatus*. Biochim. Biophys. Acta **460**:393–407.

Mustardy, L. and Garab, G. (2003). *Trends in Plant Science.*

Ong, A.S.H., and Tee E.S., (1992). *Natural sources of carotenoids from plants and oils.* Meth. Enzymol., 213: 142-167.

Oppenheimer, J.R. (1941). *Internal conversion in photosynthesis*. Phys. Rev. **60**:158.

Peterman, E. J. G., Gradinaru, C. C., Calkoen, F., Borst, J. C., van Grondelle, R., van Amerongen, H., (1997). Biochemistry, 36, 12208.

Pfander, H. (1992) Carotenoids: an overview. Meth. Enzymol., 213: 3-13

Pighin, J., (August 2003). *Capturing the sun: An exploration into the world Of plant science*: The Science Creative Quarterly.

Purves et al., (1995), Life: The Science of Biology, 4th Edition, by Sinauer Associates and WH Freeman.

Raven P., Evert R., Eichhorn S., (1999). *Biology of Plants, 6th ed.* Freeman and Company/Worth Publishers. New York, New York.

Rhee K., Morris E. P., Barber J., & Kuhlbrandt W., (1998). *Three-dimensional structure of the plant photosystem II reaction centre at 8A resolution*, Nature, Vol 396, 283-286.

Rich A., and Rich C., (2008). University of Louisville, Louisville, KY; modified by Dr. Toni Bell, Bloomsburg University.

Rothe, G.M. and Maurer, W.D., (1986). *In Gel Electrophoresis of Proteins.* IOP Publishing Limited, Bristol, England. pp.55-56.

Simidijiev, I., Barzda, V., Mustardy, L., and Garab G., (1997). *Isolation of Lamellar Aggregates of the Light-harvesting Chlorophyll a/b Protein Complex of Photosystem II with Long-Range Chiral Order and Structural Flexibility, Institute of Plant Biology,* Biological Research Center, Hungarian Academy of Sciences, Szeged, Hungary. Anal Biochem. 250, 169-175.

Simpson and von Wettstein, 1989

Staehelin, L.A., (1986). *Chloroplast structure and supermolecular organization of photosynthetic membranes.* Encyclopedia of Plant Physiology New Series 19:1-84.

Stoddard J. M, Nguyen L., Mata-Chavez H. and Nguyen K., **2007**. *TLC plates as a convenient platform for solvent-free reactions.* Chem. Commun., pp 1240 – 1241.

Thomson and Wadsworth, 2003.

Tomi T, Shibata Y, Ikeda Y, Taniguchi S, Haik C, Magata N, Shimada K, Itoh S., (2007). *Energy and Electron transfer in the photosynthetic reaction centre complex of Acidiphilium rubrum containing Zn-bacteriochlorophyll a studied by femtosecond up-conversion spectroscopy,* Vol.

van Grondelle, R., Dekker J., Gillbro T., and Sundstrom V.. (1994). *Energy transfer and trapping in photosynthesis*. Biochim. Biophys. Acta **1187**:1–65.

van Grondelle, R. and J. Amesz (1986). *Excitation energy transfer in photosynthetic systems.* In: Govindjee, J. Amesz and D.C. Fork (eds.) Light Emission by Plants and Bacteria, pp. 191- 223. Kluwer Academic, Netherlands.

van Oort B., van Hoek A., Ruban A.V, van Amerongen H., (2007). *Aggregation of light-harvesting Complex II leads to formation of efficient excitation energy traps in monomeric and trimeric complexes*. FEBS Letters 581:3528-3532.

Vengris M, PhD thesis, Promoter: Prof. Dr. R.van Grondelle (2005), *Biological photoreactions explored by multi-pulse ultrafast spectroscopy.*

Vogel A. I, Tatchell A.R, Furnis B. S, Hannaford A.J , Smith P.W.G. *Vogel's Textbook of Practical Organic Chemistry* (5th Edition) (Hardcover) by ISBN 0582462363.

Walz T. and Ghosh R., (1997). *Two-dimensional crystallization of the light-harvesting I-reaction centre photounit from Rhodospirillum rubrum,* J. Mol. Biol. **265** pp. 107–111.

Willstater, Stoll. (1928). *Investigations on Chlorophyll.* Science Press.

Zuber, H., and R.A. Brunisholz. (1991). *Structure and function of antenna polypeptides and chlorophyll-protein complexes: Principles and variability. In: Chlorophylls, ed. H. Scheer*, pp. 627–692. Boca Raton: CRC Press.